OPTIMIZATION OF TORQUE AND POWER PRODUCED FROM A SMALL SCALE VERTICAL AXIS WIND TURBINE

BY

MUDHAFAR ALI HASAN MUAHAFAR

A Thesis Presented to the

DEANSHIP OF GRADUATE STUDIES

KING FAHD UNIVERSITY OF PETROLEUM & MINERALS

DHAHRAN, SAUDI ARABIA

In Partial Fulfillment of the
Requirements for the Degree of

MASTER OF SCIENCE

In

MECHANICAL ENGINEERING

May 2018

KING FAHD UNIVERSITY OF PETROLEUM & MINERALS

DHAHRAN- 31261, SAUDI ARABIA

DEANSHIP OF GRADUATE STUDIES

This thesis, written by **MUDHAFAR ALI HASAN MUDHAFAR** under the direction of his thesis advisor and approved by his thesis committee, has been presented and accepted by the Dean of Graduate Studies, in partial fulfillment of the requirements for the degree of **MASTER OF SCIENCE IN MECHANICAL ENGINEERING.**

Dr. Haitham M. Bahaidarah
(Advisor)

Dr. Zuhair M. Gasem
Department Chairman

Dr. Ahmet Z. Sahin
(Member)

Dr. Salam A. Zummo
Dean of Graduate Studies

Dr. Hassen Ouakad
(Member)

24/5/18

Date

To

my parents,

my brothers and sisters,

my wife and daughters, Aalaa and Aseel,

For their love, encouragements, sacrifices and prayers.

ACKNOWLEDGMENTS

All praises and thanks are due to Allah for bestowing me with health, knowledge and patience to complete this work. May the peace and blessing of Allah be upon Prophet Muhammad (PBUH), his family and his companions. Thereafter, many thanks to KFUPM for granting me the opportunity to pursue graduate studies with financial support.

I acknowledge, with deep gratitude and appreciation, the encouragement, inspiration, valuable time and guidance given to me by my Advisor, Dr. Haitham Bahaidarah. Special thanks are due to committee members, Dr. Ahmet Sahin and Dr. Hassen Ouakad, for their continuous encouragement, moral support, valuable time and guidance during this research work.

Deep thanks are given to the Department of Mechanical Engineering and the other faculty members for their support and encouragement.

Finally, my heartfelt gratitude is given to my parents and beloved wife, and my children Aalaa and Aseel, who always support me with their love, patience, encouragement and constant prayers. I would like to thank my brother, sisters, and all members of my family in Yemen.

TABLE OF CONTENTS

LIST OF TABLES

LIST OF FIGURES

LIST OF ABBREVIATIONS

Symbols

AEP	:	Annual Energy Production
CF	:	Capacity Factor
Cp	:	Coefficient of performance
WB	:	Weibull Betz
WP	:	Weibull probability
HP	:	Hub power
TP	:	Turbine power
TE	:	Turbine energy
TSR	:	Tip Speed Ratio
α	:	Angle of Attack
τ	:	Wind turbine component factor
αact	:	Actual Angle of Attack
η	:	The efficiency of the wind turbine
η rated	:	The maximum efficiency of the wind turbine
β	:	Blade Pitch Angle
θ	:	Azimuth Angle (Rotor Position)
CL	:	Lift Coefficient
CD	:	Drag Coefficient
FL	:	Lift Forces (N)
FD	:	Drag Forces (N)

FT : Tangential Forces (N)

FN : Normal Forces (N)

FL, help : Useful Lift Forces (N)

FD, circ : Centrifugal Drag Forces (N)

FL, circ : Centrifugal Lift Forces (N)

FD, hurt : Hurt Drag Forces (N)

WD : Weibull Distribution

WCP : Weibull CP

TE : Turbine Energy

TP : Turbine Power

ABSTRACT

Full Name : Mudhafar Ali Hasan Mudhafar

Thesis Title : Optimization of torque and power produced from a small scale vertical axis wind turbine

Major Field : Mechanical Engineering

Date of Degree : May 2018

A small-scale vertical axis wind turbine with 2.56 m rotor diameter, 1.5 m blade length, and rotational speed of 179 r.p.m, with NASA0012 airfoils (three straight-bladed rotor) has been chosen for the present study. This thesis covers two main tasks. First, optimization of the torque and power produced from a small-scale vertical axis wind turbine. The analysis is conducted at different values of tip speed ratio ranging from 1 to 4. The blade pitch angle is kept fixed at every position of the rotor for modification I as well as being used as a function of the azimuth angles at every position of the rotor for modification II to investigate the optimum value of the fixed blade pitch angle at the optimum value of TSR. The basic idea is to simulate the motion of the blades (three-blades) when they rotate around a circle of 360o. Once the desired pitch angles and angles of attack have been acquired, the lift and drag coefficients (functions of the angle of attack and Reynolds number) can be obtained. Then, the drag and lift forces can be evaluated. Finally, the lift and drag forces can be solved to find the useful torque and

power of the model. The second task, annual energy production and capacity factor, is acquired based on the standard relationships available in the literature.

The study was carried out by varying the pitch setting angles (β) of the straight-bladed VAWT. Two scenarios for enhancing the power output of the VAWT model were used. Scenario I was used to examine the performance of the VAWT model when pitch angles (β) were kept fixed. This method ensured an important increase in the power output, and the optimum value of the blade pitch angle was 90 degrees. Scenario II was used to investigate the performance of the VAWT model when the pitch angles (β) were adjusted to be functions of the azimuth angles (θ).

The case study VAWT model tends to have a good capacity factor and an excellent annual energy production. Furthermore, the impact of wind speed on the performance and annual energy production of the selected model is more effective than the hub height.

In general, the numerical model results of the modification I were found to be in good agreement with the numerical model results from the previous studies, as the maximum deviation of model results was within 13%. In addition, a new direction (modification II) was used to improve the power output of the VAWT model and significant results were obtained as a result of using this technique.

ملخص الرسالة

الاسم الكامل: مظفر علي حسن مظفر

عنوان الرسالة : الحصول على العزم والاستطاعه الاعظميين لعنفه ريحيه ذات محور شاقولي و أبعاد صغيره

التخصص: هندسه ميكانيكيه (علوم حراريه)

تاريخ الدرجة العلمية: مايو 2018

تم اختيار عنفة ريحية صغيرة ذات محور عمودي صغير، ذوقطردوار يصل الى 2.56 (م)، وطول الشفرات 1.5 (م)، وسرعة دوران 179 (دورة في الدقيقة)، مع افتراض شفرات ناسا0012 (ثلاث شفرات) للدراسه الحاليه. هذه الأطروحة تغطي مهمتين رئيسيتين. أولا، تحسين عزم الدوران والقوة المنتجة من عنفة ريحية ذات محور رأسي وأبعاد صغيره. ويجرى التحليل بقيم مختلفة ل TSR (والتي تعرف بانها النسبه بين السرعه المحيطيه للدوار الى سرعة الريح) وتتراوح بين (1 إلى 4) ويتم اختيار زوايا الشفرات لتكون تابعه لزوايا السمت في كل موضع دوران للدوار. تتلخص الفكرة الأساسية في محاكاة حركة الشفرات (ثلاثة شفرات) عندما تدور حول دائرة من 360 درجه. بعد أن يتم تحديد واختيار زوايا الشفرات المرغوبه فانه بامكاننا حساب معاملات الرفع والسحب والتي تعتبر توابع لزوايا الشفرات ورقم رينولد. في نهاية المطاف، يتم تحديد قوات السحب و الرفع للحصول على عزم دوران وقوة مفيدة من النموذج المحدد. ثانيا، يتم تحديد إنتاج الطاقة السنوية وعامل القدرة على أساس العلاقات القياسية المتاحة في الكتب ذات العلاقه.

وقد أجريت الدراسة من خلال تغيير زوايا الشفرات (β) لنموذج عنفه ريحيه ذات محور عمودي وشفرات مسطحه. واستخدم سيناريوهان لزيادة انتاج الطاقة للنموذج. تم استخدام السيناريو الأول لدراسة أداء النموذج عندما يتم تثبيت زوايا االشفرات (β). وتستخدم مجموعة واسعة من هذه الزوايا الثابتة. وقد ضمنت هذه الطريقة زيادة هامة في انتاج الطاقة وكانت القيمة المثلى لزاوية الشفرات الثابته هي 90 درجة. واستخدم السيناريو الثاني للتحقيق من أداء النموذج المدروس عند تعديل زوايا الشفرات (β) لتكون تابعه الزوايا دوران الدوار (θ). وقد تم إنتاج زيادة كبيرة في انتاج الطاقة كتسلسل من استخدام هذا التعديل.

يميل نموذج الدراسة المختار إلى أن يمتلك عامل قدرة جيد وإنتاج الطاقة السنوية ممتازة. وعلاوة على ذلك، كان تأثير سرعة الرياح على الأداء وإنتاج الطاقة السنوية على النموذج المحدد أكثر فعالية من ارتفاع المحور.

بشكل عام، النتائج العدديه للنموذج المختار في توافق جيد مع النتائج العدديه للنموذج بنفس الابعاد من الدراسات السابقه بانحراف أقصى لنتائج النموذج في حدود 13٪. بالإضافة إلى ذلك، تم استخدام اتجاه جديد (التعديل الثاني) لتحسين إنتاج الطاقة للنموذج وتم الحصول على نتائج هامة كنتيجه لاستخدام هذه التقنية.

CHAPTER 1

INTRODUCTION

1.1 Introductory Statement

Global demand for energy has highlighted a matter of great concern about greenhouse effects caused by fossil fuels and GHG emissions. This has resulted in global heating and melting of the ice caps and has attracted an increasing use of the sustainable energy resources provided by biomass, sun, wave, and wind. Over the last 35 years, wind energy has become a prominent part of the solution to these problems, because of its low cost and availability in different sizes according to the desired purpose [1].

Wind energy is a source of producing power that is growing rapidly. According to the World Wind Energy Association (WWAE), the globally installed capacity of wind turbines grew at an average rate of 24.03GW from 2005 to 2012 [2]. According to the latest report of WWEA (2014), worldwide installed wind power capacity reached 310GW overall, and 200GW in twenty OECD countries (Organization for Economic Co-operation and Development). The growth is about 100GW in non-OECD countries. It is supposed to reach 520GW by 2035 and to about 320GW in OECD countries, while the contribution of non-OECD countries will be about 200GW by the same year. The annual growth in installed capacity of the wind power in the world, OECD and non-OECD

countries is presented in Fig 1.1. The Annual Worldwide Wind Energy Capacity in the total installed capacity is presented in Fig 1 and Fig 2.

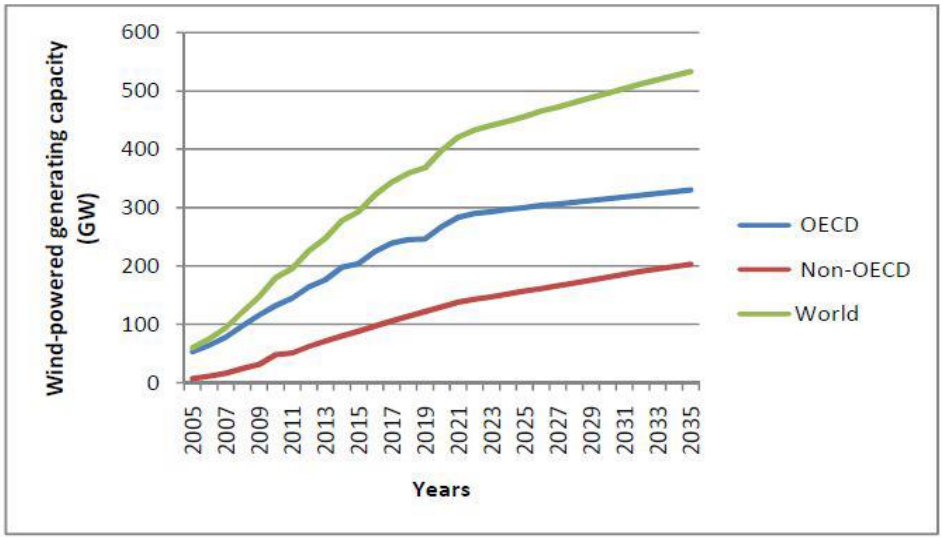

Figure 1.1: Yearly wind energy capacity throughout the world [2]

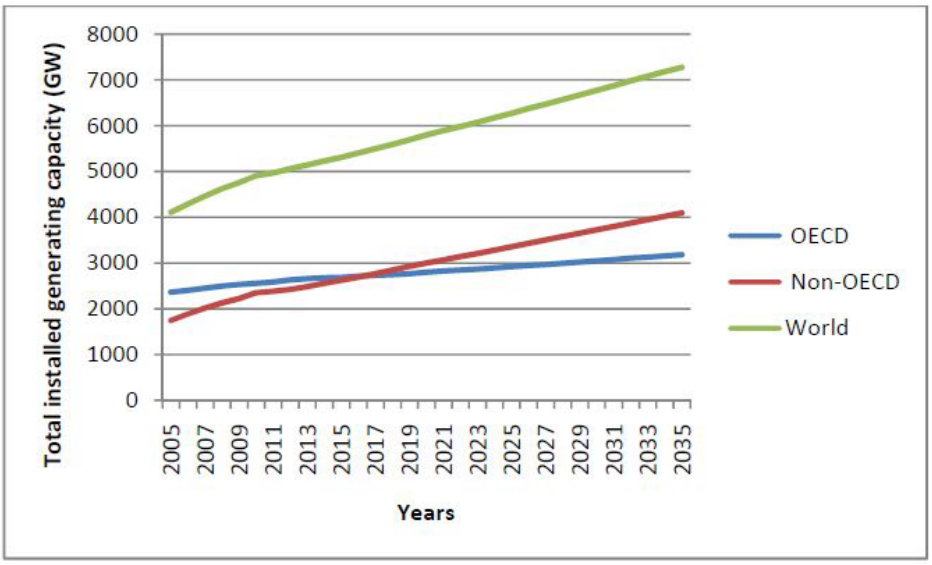

Figure 1.2: Yearly total installed capacity throughout the world. [2]

Wind turbines are either horizontal axis wind turbines (HAWT), or vertical axis wind turbines (VAWT) according to the practical method of power generation. They have basic components such as a base, tower, generator, gearbox, yaw engine, rotor, control system, and a transformer. In HAWT, where the rotor axis is parallel to the ground and the blades rotate around it, the rotors and generators are at the highest point of the tower and should be pointed into the wind. HAWT are used in commercial applications. In VAWT, the rotor shaft is vertical, and the blades rotate around it. VAWT has the advantage that it can deliver flow from all directions. Thus, a yaw drive mechanism, which is an expensive component used in HAWT, is not needed in this type [3].

1.2 Research Objectives

The overall objective of the proposed work is to study a small-scale vertical axis wind turbine (using small sizes of dimensions and capacity) at different values of TSR. Two scenarios for an enhanced power output of the VAWT model were used. Scenario I examines the performance of the VAWT model when pitch angles (β) are kept fixed. Scenario II investigates the performance of the VAWT model when the pitch angles (β) are adjusted to be functions of the azimuth angles (θ). The study will concentrate on exploring the appropriate design of a vertical axis wind turbine. The annual energy production and capacity factor will be investigated. The pitch angles at every position of the rotor around a circle will be determined to find these angles, as well as the angles of attack. The corresponding lift and drag forces will be solved from the relationships available in the literature. The specific objectives of this research are:

1. To study and analyze a small-scale vertical axis wind turbine at different values of TSR in two scenarios of the variation of the pitch angles.
2. To determine the optimum pitch angles and angles of attack at every position of the rotor around a circle of 360^{o}.
3. To estimate drag and lift coefficients corresponding to the calculated angles of attack mentioned in objective 2.
4. To calculate drag and lift forces at every position of the rotor.
5. To find any forces affecting the motion of the rotor around a circle of 360^{o}.
6. To calculate the torque and power based on the useful forces at a wide range of Tip Speed Ratio (TSR) and pitch angles.
7. To estimate the optimum values of power and torque produced from this small-scale vertical axis wind turbine based on the analysis.
8. To determine the power curve and Weibull distribution of the wind turbine under consideration based on the wind turbine database.
9. To investigate the parameters which affect the annual energy production and capacity factor of the wind turbine.

1.3 Structure of the thesis

This thesis consists of five chapters. In Chapter 2, the literature review of the previous work and the significance of this study are discussed in detail. The methodology of this study in both tasks (optimization of torque and power produced from a small scale VAWT as well as evaluation of annual energy production and capacity factor) are

discussed in chapter 3. In Chapter 4, the results are presented and discussed in detail. Chapter 5 summarizes the conclusion, recommendation and the future work.

CHAPTER 2

LITERATURE REVIEW

2.1 Introduction

In this chapter, the literature review will be carried out to overview the previous research work related to wind turbine analysis. This study provides the guidelines and techniques that will help in achieving the objectives of this thesis.

2.2 Extracted torque and power from a wind turbine

Due to rapid changes in wind speed, the power captured by a wind turbine varies continuously. Such operations are highly undesirable and need controllers. Therefore, in order to achieve the best performance of a wind turbine, there is a need to modify its design [4]. Researchers have paid more attention to the pitch blade control to optimize the torque and power from the wind turbine, to choose the best Tip Speed Ratio and pitch angle that ensure maximum torque without noise and vibration while rotating.

The problem of the wind turbine is associated with the design of the wind turbine itself. Some of the wind turbine designs are too big to harness more energy from the wind. Some of the researchers have started to harness the power from wind by designing a small wind turbine which can operate at low wind speeds with a low Reynolds number [5]. However, it might be impossible to make the rotor spin and harness significant energy, due to the low wind speed [6].

Different small wind turbine models have been tested in wind tunnels in order to characterize the performance of wind turbines under various wind conditions [7]. In 2005, a fixed-pitch fixed-speed wind turbine model of 0.7 m rotor diameter was built and tested in a wind tunnel at the University of Stuttgart [8]. In the same year, another wind turbine model with a rotor diameter of 0.54 m was built at the University of Applied Sciences in Lübeck [9], where the pitch angle was controlled automatically using a stepper motor, and the model operated at a fixed-speed mode. In 2006, a new model was developed at the Technical University of Berlin [9]. The model had a rotor diameter of 0.7 m; however, the model was restricted by only four different pitch angles (0°, 2.5°, 5°, 10°)[10], where each time the angle had to be set manually before the test took place. In 2008, the same model was modified and reconstructed at the Technical University of Berlin [11]. A major difference (compared to the previous model) was that the pitch angle could be set manually at eight different values (0°, 1,25°, 2.5°, 3,75° 5°, 7.5°, 10°, 15°)[12], which allowed the testing to be done at more angles of attack, and therefore having better characterization for the wind turbine model. Furthermore, the project [13] improved the wind turbine's efficiency by replacing the previous blades with new ones.

Yann Staelens, Farooq Saeed, and Ion Paraschivoiu [14] have studied a model for a small-scale wind turbine with 13.8m/s as a wind speed and a rotational speed of 125r.p.m. They selected the NASA0015 two-bladed airfoil for their analysis to optimize the power and torque for their model, using CARDAAV code. See Figure 3.

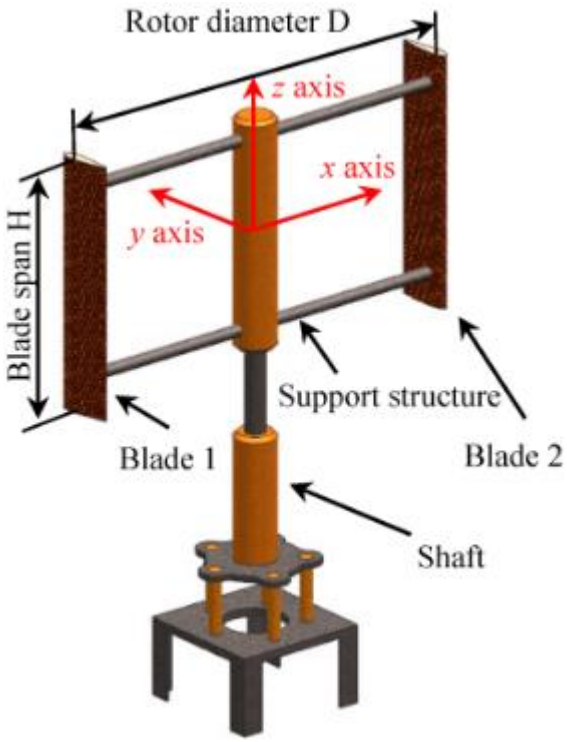

Figure 2.1: The model for the previous study for a small scale vertical axis wind turbine with two blades

They analyzed their model using three modifications to maximize the power generated from the wind turbine. The first investigation was at lower values of angle of attack (AOA); they found that the power was relatively increased, but the desired values of AOA could not be achieved. The second investigation was by choosing larger AOA above stall to observe the enhancement in power; this procedure decreased the effective angle of attack with a slight decrease in wind turbine power. Also, they noted that this value of AOA caused fatigue. The third achievement was by using the procedure of variations of AOA while rotating. However, the power extracted from this modification was less than the two previous procedures.

Javier Castillo [15] focused on a small scale of VAWT of 529.2Watts with a rotor diameter of 2m, blade length of 2m, coefficient of power of 0.17, rotational speed of 114.59 r.p.m and the blade airfoil chosen was NASA0012 with three and four blades to compare between them in terms of performance for his design. He investigated whether a three-blade was better than four-blade designs since it was more effective and efficient. In addition, he proved that a rotor with a large diameter is more efficient than a smaller one at the same rotational speed. He discovered that increasing the tangential wind speed led to a smaller angle of attack, a larger Reynolds number and a larger lift coefficient. One of his recommendations was that an experimental test for his model was needed to validate his results.

S. B. Weiss, 2010 [16] analyzed a small-scale vertical axis wind turbine for three and four blades and assumed that pitch angles could be half of the rotor position and optimized torque and power according to his assumption. See Fig 4. However, the drawback of this research was that he only focused on one value of tip speed ratio, viz. 0.3. Therefore, the research in this domain needs deeper work at the wide range of tip speed ratios (TSR) to decide which value of TSR is the best for the selected model. Accordingly, in our analysis, we will choose this assumption and enhance it by analyzing the selected model at a wide range of TSR and pitch angles which are functions of rotor position [17].

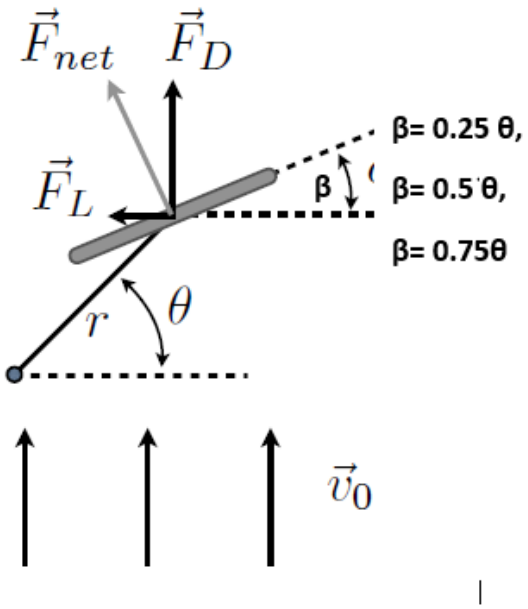

Figure 2.2: Blades description as they rotate, and the corresponding drag and lift forces

Jon De Coste et al [18] analyzed a model of a small-scale vertical axis wind turbine at a wind speed of 6 m/s and rotor diameter of 2.56 m with three rotor blades, and the NASA0012 airfoils were chosen at different values of TSR and at different values of blade pitch angles to see the best design for their model. The model was carried out at a wide angle of TSR and pitching angle to simulate the motion of the rotor at different values of pitching angles and angles of attack [19]. They investigated that the torque and power could be maximized according to the chosen TSR and pitch angle. However, this did not provide a clear procedure to show how results were achieved. Therefore, in this study, we will choose this model with the same parameters and implement a code to obtain results that optimizes the torque and power of a small-scale vertical axis wind

turbine [20], and we will validate our results with the mentioned model as shown in Figure 4.

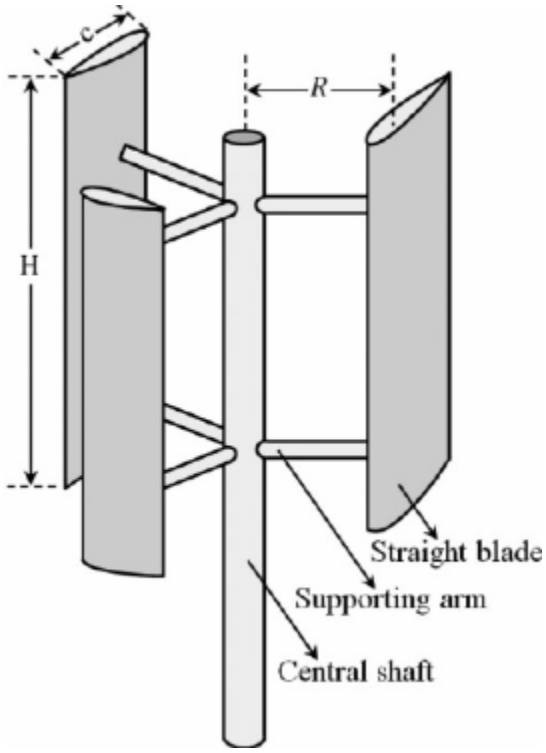

Figure 2.3: The selected case study model (straight- bladed VAWT): three blades with c=0.07m, r=1.28m, and h=1.5m

2.3 How a wind turbine works

The wind consists of two main driving forces on the turbine blades - drag and lift forces. If the wind on the lower side of the wind is greater than the wind on the opposite side, then the force will be produced [21]. The velocity difference will cause the difference in pressure, where the pressure in the leeward side is higher than the pressure in the windward side. The low pressure on the leeward side will pull the airfoil to that

side. This concept is called the Bernoulli's concept [22]. The components of lift and drag forces are the vectors parallel and perpendicular to the relative wind [23], as shown in Fig 2.4.

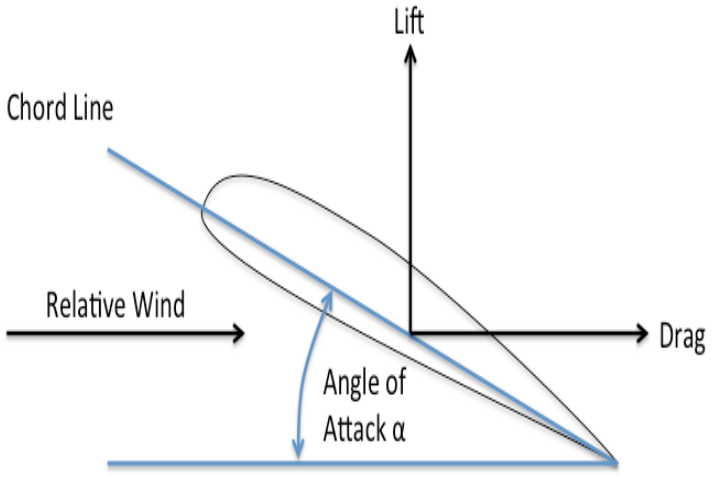

Figure 2.4: Force vector on an airfoil

2.4 The Betz Law

The basic idea of the wind turbine is to extract energy from wind to generate power. However, it cannot extract 100% of energy into work, since there are losses such as mechanical losses that limit the wind turbine's capability to convert all the energy into work [24]. Betz's Law gives us the maximum power that can be produced from the wind turbine in practical operation. The coefficient that gives us an ideal power is called the power coefficient or Betz Limit. The ideal value of this coefficient is 16/27 or 0. 593. However, in real life, this coefficient does not exceed 0.48. Figure 6 shows the coefficient of power for different types of wind turbine [25].

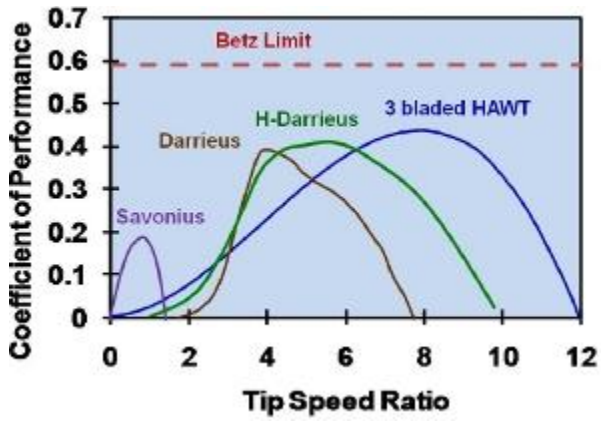

Figure 2.5: Coefficient of power for different types of wind turbine at different values of tip speed ratio [26]

2.5 Tip Speed Ratio (TSR)

The better the match between the angular velocity of the rotor and wind speed, the better the efficiency will be. Therefore, a good design of wind turbine is very significant to obtain optimum efficiency, torque and power. The rotating of the rotor should be balanced to avoid entering the wind between gaps in blades when slow-rotating, and to avoid the high solidity of the blades in rapid-rotating, which reduces the power produced from the wind turbine. Accordingly, the optimum TSR has to be kept obtaining maximum power and torque extracted from the wind turbine. In practice, the high value of TSR is desirable to get more power produced. However, a high value of TSR will cause vibration, noise and erosion, which may cause failure and even destruction [27]. The general equation of TSR can be expressed as follows:

$$TSR = \frac{u}{v} = \frac{\omega \times r}{v} \quad \text{..... (2.1)}$$

where u_b is the blade speed (m/s), r is the rotor radius (m), u is the wind speed (m/s), and w is the angular velocity (rad/sec) [28].

2.6 Solidity of wind turbine

Solidity is a function of TSR and this factor determines the structural design of the rotor, generator speed, and gear ratio. This factor is used to find the chord length of the blade. The total area of the rotor equals the solidity times frontal area of the rotor. The individual blade area is the total area over a number of blades. Finally, the chord length equals the individual area over the hub height of the rotor. The relationship between Solidity and TSR is shown in Figure 7, [29].

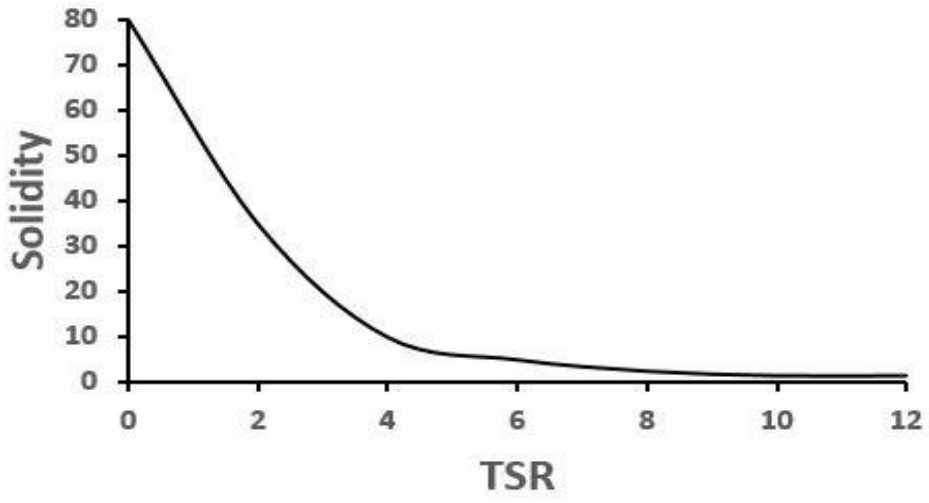

Figure 2.6: The relationship between TSR and Solidity

2.7 Power curve

The total amount of power a wind turbine generates over an annual average wind speed is called power curve data. The power curve is very important to know the wind turbine health and performance. The common relationship for power curve calculation is given by:

$$E_v = 8760 \times \sum_{x=0}^{25} P_X P(x) \quad \text{..... (2.2)}$$

Where: P_x is the turbine energy at x velocity, P(x) is the Weibull probability, and Ev is the power curve data.

The power curve contains three basic regions. (1) Cut-in speed is where the turbine starts to produce power (around 3-3.5 m/s) and below this speed, the power extracted from the wind turbine is zero. (2) Rated power output is when the wind turbine reaches its optimum value and the velocity of the wind in this region is around 12-17 m/s. (3) Cut-out wind speed is when the wind turbine should be stopped to avoid the destruction of its blade and the velocity is around 23-25 m/s. Figure 8 shows these three regions in detail [30].

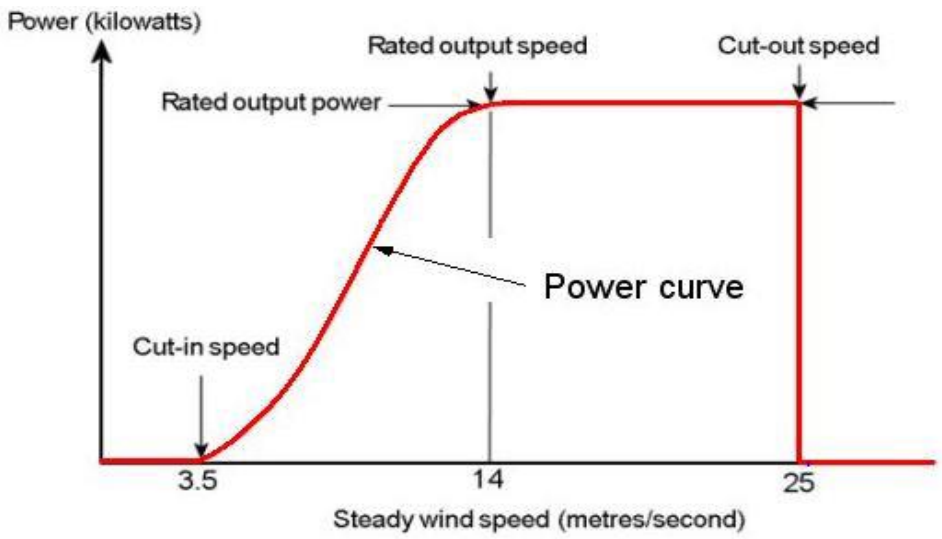

Figure 2.7: The standard power curve for a wind turbine [13].

2.8 Weibull distribution

The Weibull probability can be defined as the probability of a wind to achieve x velocity over an annual study [31]. A Weibull distribution of wind speed is calculated after long-term study of annual wind speeds during the year for a case study region. The Rayleigh wind speed distribution is a special case of Weibull distribution with the shape factor equal to 2.

The following relationship is to calculate a Weibull distribution over a wide range of annual mean wind speeds [32].

$$P(x) = (\frac{k}{c})(\frac{x}{c})^{k-1} \exp[(-\frac{x}{c})^{k}] \quad \ldots\ldots (2.3)$$

Where: k is the shape factor, k= (1-3). If the shape factor is higher, then the wind speed distribution is wide and if smaller, then the wind speed distribution is narrow. x is the wind speed velocity at a wide range of annual study and ranges from 0 to 25 m/s. c is the scale factor which should be higher than zero. The scale factor can be calculated from the following equation [33]:

$$c = \frac{\bar{v}}{\Gamma(1+\frac{1}{k})} \quad \text{..... (2.4)}$$

Where: Γ is the Gamma function, k is the shape factor, and v^- is the annual mean speed (m/s). The Weibull distribution of the model case study is shown in Figure 9.

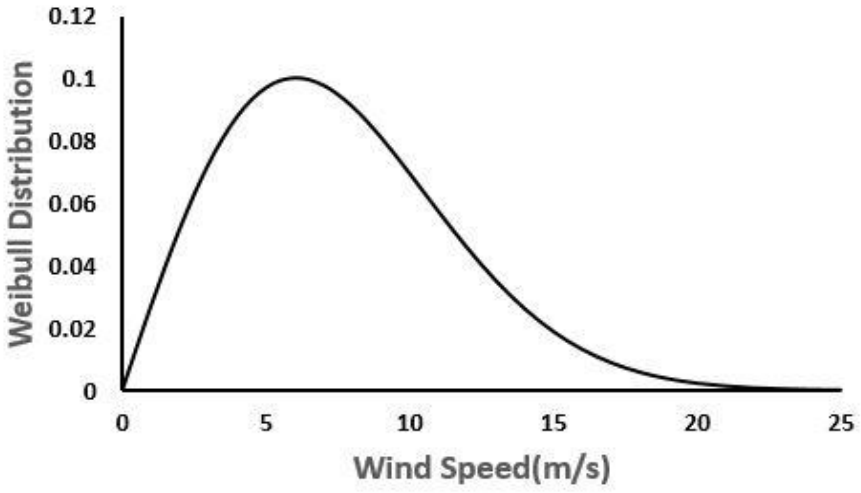

Figure 2.8: The Weibull Distribution versus wind speed for the selected model

2.9 Annual Energy Production (AEP) and Capacity Factor (CF)

The net AEP is the energy output that can be produced from a wind turbine at a given annual average wind speed. The gross AEP considers the effect of many factors such as coefficient of power, mechanical and electrical conversion losses, blade soiling losses, array losses, and machine availability. Capacity factor can be defined as the ratio of actual energy produced by the system annually to annual system energy at a constant rated power [34]. The following relationship can be used to calculate AEP as follows [35]:

$$AEP = \sum TE \times (1 - AL) \times (1 - ML) \times (8760 \times AV) \quad \text{..... (2.5)}$$

Where: TE is the turbine energy (kW), AL is the array losses, Ml is the miscellaneous losses, and AV is the machine availability.

The capacity factor can be calculated as follows [10]:

$$CF = \frac{AEP}{8760 \times P_{Rated}} \quad \text{..... (2.6)}$$

2.10 Angle of attack and pitch angle

The angle between the tangential line and blade path is called the pitch angle. The angle between the chord length of the blade and relative wind speed is called angle of

attack. This angle is very important to determine the type of flow over an airfoil. There are four situations for different values of angles of attack which display the stall and separation for every case.

At the angle of attack of 5^{o} a slight separation occurs. At the angle of attack of 15^{o}, the flow remains attached on both sides. At 25^{o} the flow reaches stall conditions where the pressure is equal on both top and bottom sides, as shown in Figure 2.9.

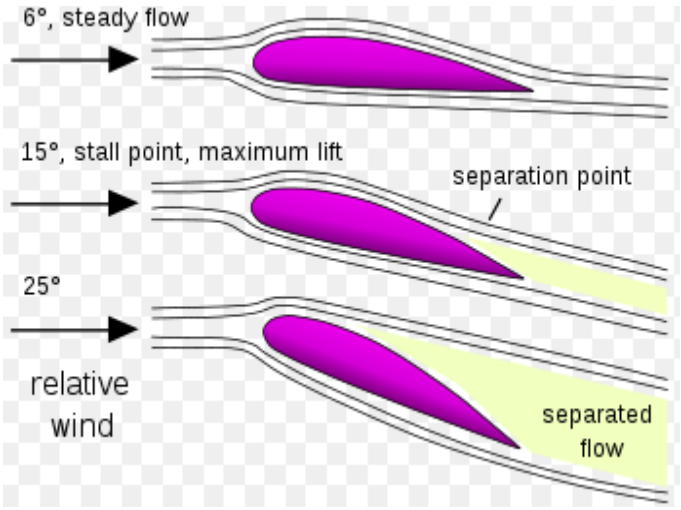

Figure 2.9: Three scenarios of the angle of attack of an airfoil

.

2.11 Significance of this research

The literature review, most cited in the previous section, illustrates that several studies have been achieved in terms of optimizing power and torque from a small-scale vertical axis wind turbine for fixed pitch angles. However, several aspects, such as the best position and the best TSR for moving pitch angles around a circle for the selected model have not been well defined, and only S. B. Weiss, 2010 analyzed moving pitch angles of

0.5 of the rotor position at one value of TSR. Thus, there is a gap in this analysis which requires deep study and analysis for moving pitch angles at a wide range of TSR to investigate the best values that ensure maximum power and torque are extracted from the selected model. Consequently, there is an urgent need to study the maximum power, torque, and performance of a vertical axis wind turbine at every condition and at every location to ensure maximum annual energy production for a wind turbine.

CHAPTER 3

METHODOLOGY OF THE RESEARCH

3.1 Introduction

This chapter outlines the mathematical and numerical analysis of the blade pitch angles and the angles of attack to fulfill the objectives of the present study. In this study, the steps of calculating power and torque produced from a small-scale vertical axis wind turbine are evaluated. Also, the annual energy production and capacity factor of the selected model is evaluated by following many steps to achieve this aim.

3.2 Methodology of calculating extracted torque and power from a small scale vertical axis wind turbine

In our analysis, the angles of attack change around a circle from 0-360^{o} and we must implement a code and resolve and arrange the results in an Excel spreadsheet to determine the value of every pitch angle at every position of the rotor angle.

Two scenarios for an enhanced power output of the VAWT model were used. Scenario I examines the performance of the VAWT model when the pitch angles (β) are kept fixed. Scenario II investigates the performance of the VAWT model when the pitch angles (β) are adjusted to be functions of the azimuth angles (θ). Because the attention of

this research is on a VAWT straight – bladed model (see Fig. 3.1), the priority of the governing equations can be presented as follows:

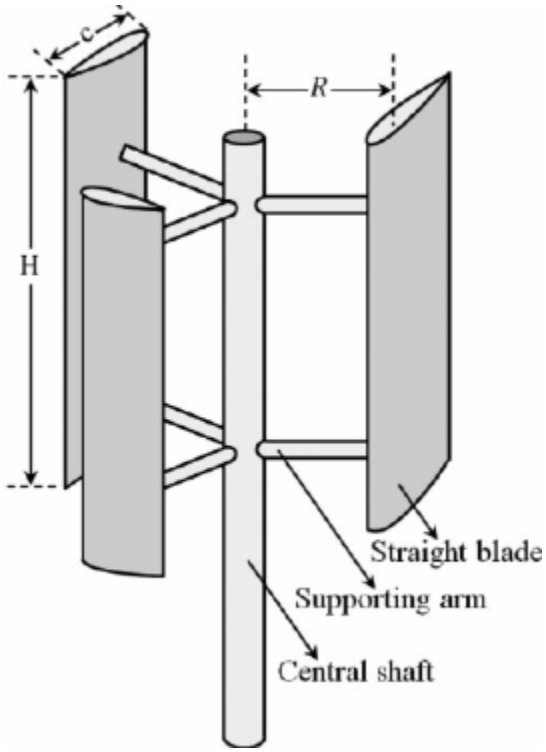

Figure 3.1: The straight- bladed VAWT model

1. Discretize the domain (circle) into 72 grids starting from 0:5:360^{o}.
2. Calculate the angle of attack from the geometric presented in Figure 3.2 as follows:

$$\alpha = \arcsin\left(\frac{\cos\theta}{\sqrt{(TSR-\sin\theta)^2+\cos^2\theta}}\right) \quad \text{..... (3.1)}$$

Where: TSR is the tip speed ratio (1 – 4) and θ is the azimuth angle.

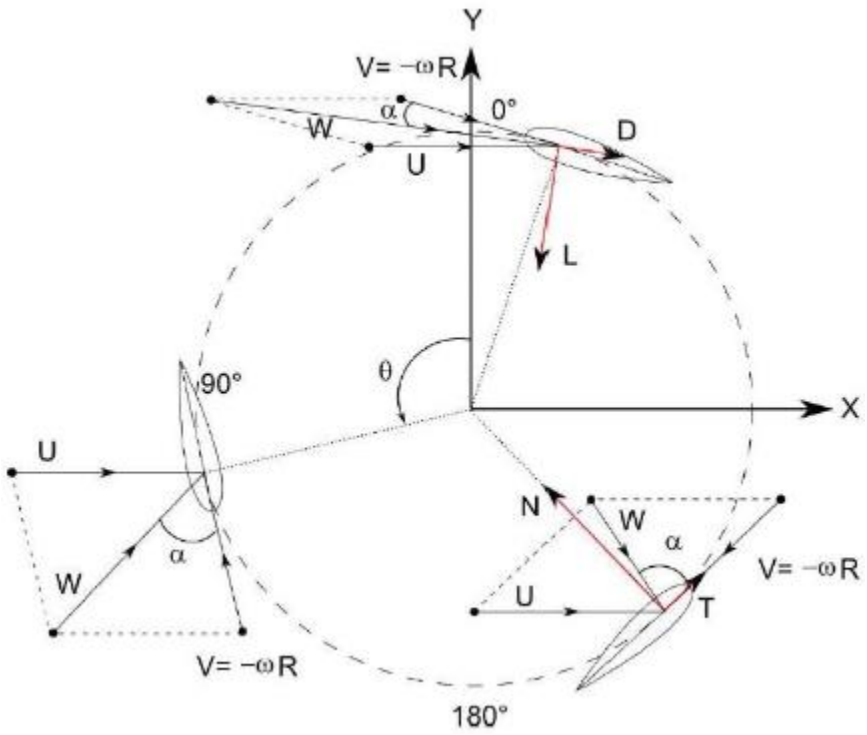

Figure 3.2: The forces and velocities on an airfoil around a circle

3. Calculate relative wind speed from the relationship [3]

$$W = \sqrt{U^2 \times [(TSR - \sin\theta^2)^2 + \cos\theta^2]} \quad \text{.....} \quad (3.2)$$

where U is the constant wind speed, 6 m/s.

4. The expression for Reynold's Number can be calculated from the relationship:

$$R_E = \frac{TSR \times W \times \rho_{air} \times cl}{\upsilon_{air}} \quad \text{.....} \quad (3.3)$$

where: TSR is the tip speed ratios (1 – 4), W is the relative wind speed (m/s), ρ_{air}, and υ_{air} are the air density and air viscosity of 1.205 kg/m^3 and 1.81×10^{-5} N s/m^2.

5. The lift and drag coefficients C_L and C_D can be determined by interpolating known experimental data for NASA0012 using both Reynold's Number and angles of attack relationships.

6. Calculate lift and drag forces from the following equations:

$$F_L = \frac{1}{2}\rho \times W^2 \times bl \times cl \times C_L \quad \text{..... (3.4)}$$

$$F_D = \frac{1}{2}\rho \times W^2 \times bl \times cl \times C_D \quad \text{..... (3.5)}$$

Where: ρ_{air} is the density of air of 1.205 kg/m^3, W is the average relative wind speed (m/s), bl is the blade length of 1.5 m, cl is the chord length of 0.07 m, and C_L and C_D are the lift and drag coefficients.

7. Calculate the force in the direction of the rotation and centrifugal force as follows:

$$F_{L,help} = F_L \times \cos\left((\frac{\pi}{2}) - (\frac{\alpha_{act} \times \pi}{180})\right) \quad \text{..... (3.6)}$$

$$F_{L,circ} = F_L \times \sin\left((\frac{\pi}{2}) - (\frac{\alpha_{act} \times \pi}{180})\right) \quad \text{..... (3.7)}$$

$$F_{D,hurt} = F_D \times \cos\left(\frac{\alpha_{act} \times \pi}{180}\right) \quad \text{..... (3.8)}$$

$$F_{D,circ} = F_D \times \sin\left(\frac{\alpha_{act} \times \pi}{180}\right) \quad \text{..... (3.9)}$$

Where: $F_{L,\,help}$ is the force in the direction of rotation, $F_{L,\,circ}$ is the centrifugal force, $F_{D,hurt}$ is the force in the opposite direction of the rotation, $F_{D,circ}$ is the centrifugal drag

force, and α_{act} is the actual angle of attack after considering the added pitch angles (rad).

8. The useful (parallel) force and perpendicular (normal) force can be found from the following relationships:

$$F_T = F_{L,help} - F_{D,hurt} \quad \text{(3.10)}$$

$$F_N = F_{L,circ} + F_{D,circ} \quad \text{(3.11)}$$

Where: $F_{L,help}$ is the force in the direction of rotation, $F_{L,circ}$ is the centrifugal force, $F_{D,hurt}$ is the force in the opposite direction of the rotation and $F_{D,circ}$ is the centrifugal drag force.

9. Finally, calculate the extracted torque and power from the following relationships:

$$TORQUE = F_T \times r \quad \text{(3.12)}$$

$$POWER = TORQUE \times \omega \quad \text{(3.13)}$$

Where: r is the rotor radius of 1.28 m and ω is the angular velocity of 18.745 rad/sec.

3.3 Methodology of calculating annual energy production (AEP) and capacity factor (CF)

There are several steps used to determine AEP which can be summarized as follows:

1. Find power for the selected wind turbine at every value of wind speed (0-25 m/s) from the power curve data. The total amount of power a wind turbine generates

over an annual average wind speed is called power curve data. The power curve is very important in determining the wind turbine health and performance. The power curve contains three basic regions: (1) Cut-in speed, where the turbine starts to produce power (around 3-3.5 m/s) and below which the power extracted from the wind turbine is zero. (2) Rated power output, when the wind turbine reaches its optimum value; the velocity of the wind in this region is around 12-17 m/s. (3) Cut-out wind speed, when the wind turbine should be stopped to avoid the destruction of the wind turbine blade; the velocity at this point is around 23-25 m/s.

2. Calculate the mean speed from the equation:

$$V_{mean} = V_{annual} \times \left(\frac{H_{hub}}{10} \right)^{\tau} \quad \text{.....} \quad (3.13)$$

Where: V_{annual} is the annual wind speed for the case study position, in our study chosen to be 6 m/s, H_{hub} is the height of the hub=3 m, and τ is the coefficient of wind turbine components (τ =0.143).

3. Determine wind speed distribution for the chosen wind turbine by using a Weibull distribution. The Weibull probability can be defined as the probability of a wind to achieve x velocity at annual study. The Weibull distribution of wind speed is calculated after long-term study of annual wind speeds during the year for a case study region. The Rayleigh wind speed distribution is a special case of a Weibull distribution with the shape factor = 2. The relationships (3) and (4) were used to calculate the Weibull distribution over a wide range of annual mean wind speeds.
4. Calculate Weibull Betz from the equation:

$$WB = \frac{1}{2}\rho \times \frac{\pi d^2}{4} \times V^3 \times WP \times (\frac{16}{27}) \quad \text{..... (3.14)}$$

Where: ρ is the air density of 1.225 kg/m^3, d is the rotor diameter of 70 m, WP is the Weibull Probabilities calculated from step 2, and V is the wind speed (0-25 m/s).

5. Calculate Weibull Cp from the relationship: [4]

$$W_{CP} = \frac{1}{2}\rho \times \frac{\pi d^2}{4} \times V^3 \times WP \times C_P \times \eta \quad \text{..... (3.15)}$$

Where: C_P is the power coefficient of 0.2 and η is the turbine efficiency which can be determined from the relationship: [4]

$$\eta = \frac{\frac{P}{P_{Rated}} - \left(\text{constant} + \textit{l}\text{inear} \times \frac{P}{P_{Rated}} + \text{quadratic} \times (\frac{P}{P_{Rated}})^2 \right)}{\frac{P}{P_{Rated}}} \quad \text{..... (3.16)}$$

where constant refers to losses that are constant and independent of power level, such as constant-speed motor/generator, constant speed pumps and fans, and can be taken as 2 %, linear refers to losses that change linearly with power level such as a fan whose speed is proportional to temperature difference and switching loss in a converter whose switching frequency is proportional to load, and it can be chosen to be 5 % , and quadratic refers to losses that change with power level squared such as copper losses at constant voltage that follow the familiar I2R formula. Others can include lubrication losses in a variable-speed gearbox, which in this formula can be taken as zero [36].

$$P_{Rated} = \frac{1}{2} \times \eta_{Rated} \times C_P \times \rho \times V^3 \times \frac{\pi \times d^2}{4} \quad \text{..... (3.17)}$$

Where η_{rated} =0.925 [6].

6. Calculate hub power (HP) from the relationship:

$$HP = \frac{1}{2}\rho \times \frac{\pi d^2}{4} \times V^3 \times C_p \quad \text{..... (3.18)}$$

7. Calculate turbine power (TP) from the relationship:

$$TP = HP \times \eta \quad \text{.....(3.19)}$$

8. Calculate turbine energy (TE) from the relationship:

$$TE = TP \times WP \quad \text{.....(3.20)}$$

9. Finally, calculate annual energy production (AEP) and capacity factor (CF). The net AEP is the energy output that can be produced from a wind turbine at a given annual average wind speed. The net AEP considers the effect of many factors such as power coefficient, losses such as blade soiling losses, array losses and miscellaneous losses, and machine availability. Capacity factor can be defined as the ratio of yearly actual energy produced by the plant to yearly plant energy at a constant rated power. The relationships (2.5, 2.6) were used to calculate AEP and CF.

CHAPTER 4

RESULTS AND DISCUSSION

4.1 Introduction

This chapter presents the results of the mathematical and numerical analysis conducted on the selected vertical axis wind turbine and its cases. Broadly speaking, the data developed fall into the following categories:

1. The results of calculating maximum torque and power of the chosen model over a wide range of pitch angles and tip speed ratios.
2. The results of determining annual energy production and capacity factor of the selected model following steps mentioned in chapter 3.

4.2 Results of calculating torque and power of a small-scale wind turbine in different scenarios

The results in this section were conducted over a wide range of tip speed ratios (TSR) ranging from 1 to 4 and the pitch angles were analyzed using two techniques: (1) The improvement of torque and power by assuming that the pitch angles are fixed, including the pitch angles of 0, 22.5, 45, 67.5, 90, 112.5, 135, 157.5, and 180 degrees throughout the revolution of the cycle from 0º to 360º. (2) The enhancement of torque and power produced from a small-scale vertical axis wind turbine by varying the blade's pitch angles

and by taking the functions of the azimuth angles. Different scenarios for improvement of the torque and power from this technique can be analyzed.

4.2.1 Results of the first technique at TSR ranging from 1 to 4 and fixed pitch angles

The study is carried out at different fixed pitch angles including the angles of 0, 22.5, 45, 67.5, 90, 112.5, 135, 157.5, and 180 throughout the revolution of the cycle from 0º to 360º.

4.2.2 Results at TSR ranging from 1 to 4 and pitch angle fixed at 0º

In order to improve the performance of the model, the blade pitch angles must be adjusted to investigate its optimum value. The total extracted average torque from the analyzed model of the three blades for this scenario is -3.243 [N.m] at TSR=1, -4.742 [N.m] at TSR=2, -5.958 [N.m] at TSR=3, -3.427 [N.m] at TSR=4, and the corresponding average produced power is -59.5 [W] at TSR=1, -86.9 [W] at TSR=2, -109.3 [W] at TSR=3, and -62.9 [W] at TSR=4. The results imply that the torque and power are negative, which means that they are opposite to the path flow; thus, this scenario is not used in practice. The summary of the results is presented in Table A.1, Appendix A.

The lift and drag forces used as well as the produced torque and power are presented in the following figures. In Figure 4.1, the lift forces are higher than the drag forces.

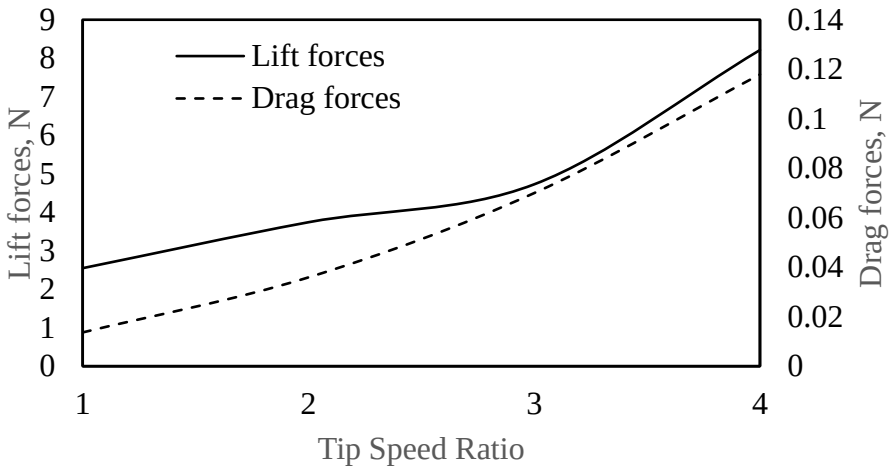

Figure 4.1: The lift and drag forces at TSR=1, 2, 3, 4 and pitch angle of 0^{o}

In Figures 4.2 and 4.3, the total extracted average torque is -3.243 [N.m] at TSR=1, -4.742 [N.m] at TSR=2, -5.958 [N.m] at TSR=3, -3.427 [N.m] at TSR=4 and the corresponding average produced power is -59.5 [W] at TSR=1, -86.9 [W] at TSR=2, -109.3 [W] at TSR=3, and -62.9 [W] at TSR=4. The results imply that the torque and power are negative, which means that hurt drag forces are higher than useful lift forces; thus, this scenario is not used in practice.

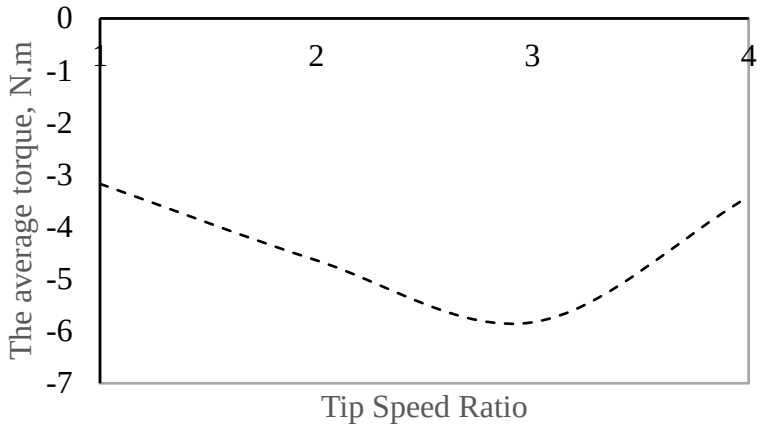

Figure 4.2: The total average torque at TSR=1, 2, 3, and 4 at pitch angle of 0º

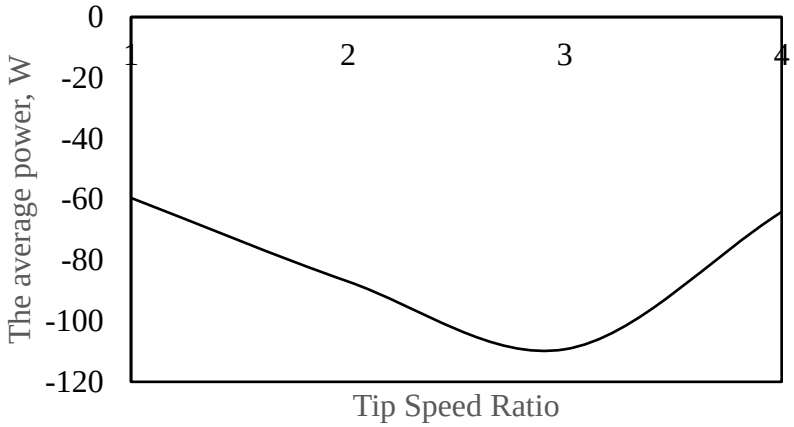

Figure 4.3: The total average produced power at TSR=1,2,3, and 4 at pitch angle of 0º

4.2.3 Results at TSR ranging from 1 to 4 and pitch angle fixed at 22.5º

The obtained results show that the produced torque and power are fluctuating according to the fixed pitch angles. The total average torque from the analyzed model of the three blades for this scenario is -2.475 [N.m] at TSR=1, -0.125 [N.m] at TSR=2, 4.316 [N.m] at TSR=3, 18.344 [N.m] at TSR=4, and the corresponding average produced

power is -45.405 [W] at TSR=1, -2.285 [W] at TSR=2, 79.181 [W] at TSR=3, and 336.526 [W] at TSR=4. The summary of the results is presented in Table A.2, Appendix A.

The lift and drag forces and used as well as the produced torque and power are presented in the following figures. The desired values of lift forces are higher than drag forces, as shown in Figure 4.4.

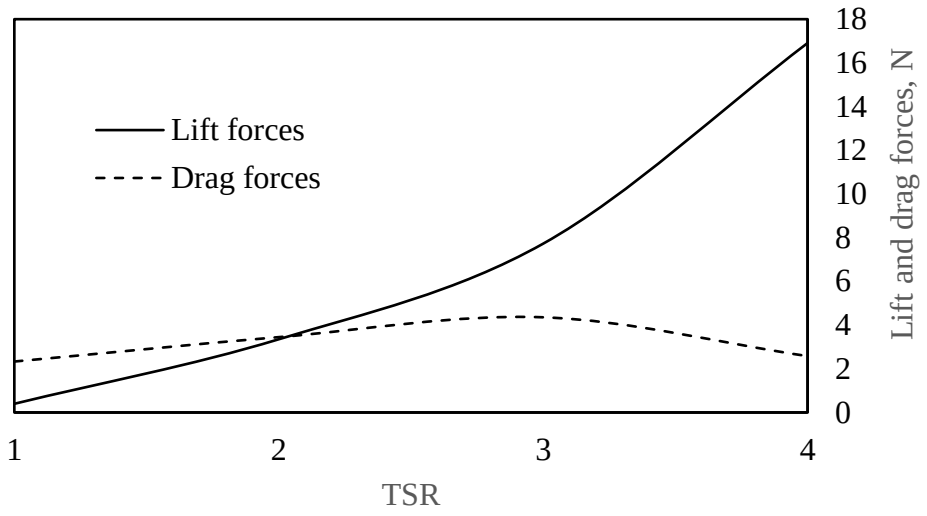

Figure 4.4: Lift and drag forces at TSR=1, 2, 3, 4 and pitch angle of 22.5^{o}

In Figures 4.5 and 4.6, the total average torque is -2.475 [N.m] at TSR=1, -0.125 [N.m] at TSR=2, 4.316 [N.m] at TSR=3, 18.344 [N.m] at TSR=4, and the corresponding average produced power is -45.405 [W] at TSR=1, -2.285 [W] at TSR=2, 79.181 [W] at TSR=3, and 336.526 [W] at TSR=4.

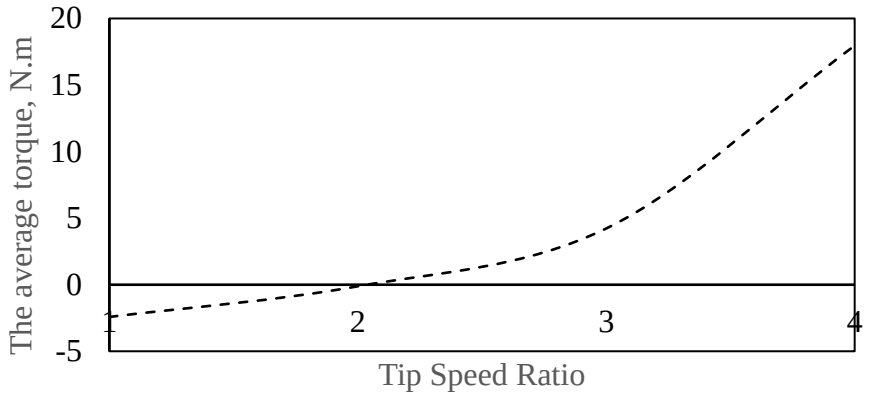

Figure 4.5: The total average torque at TSR=1, 2, 3, and 4 at pitch angle of 22.5^{o}

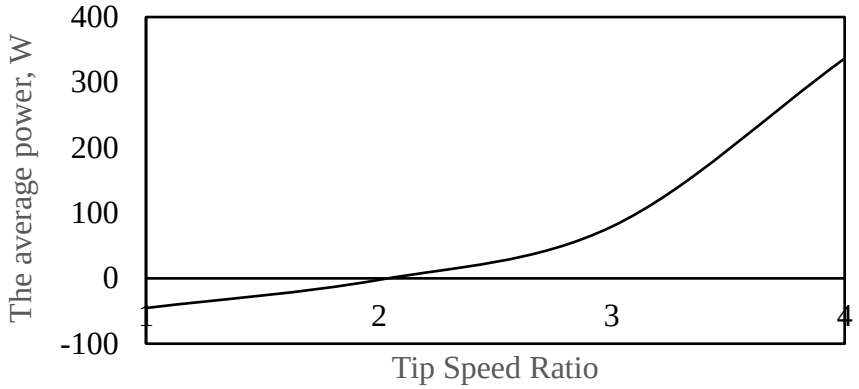

Figure 4.6: The total average produced power at TSR=1,2,3, and 4 at pitch angle of 22.5^{o}

4.2.4 Results at TSR ranging from 1 to 4 and pitch angle fixed at 45^{o}

The obtained results show that the produced torque and power are changing as the fixed pitch angles change. The total average torque from the analyzed model of the three blades for this scenario is -1.330 [N.m] at TSR=1, 4.511 [N.m] at TSR=2, 13.934 [N.m] at TSR=3, 37.324 [N.m] at TSR=4, and the corresponding average produced power is -

24.407 [W] at TSR=1, 82.762 [W] at TSR=2, 255.613 [W] at TSR=3, and 684.708 [W] at TSR=4. The summary of the results is presented in Table A.3, Appendix A.

The lift and drag forces used as well as the produced torque and power are presented in the following figures. The desired values of lift forces are higher than drag forces, as shown in Figure 4.7.

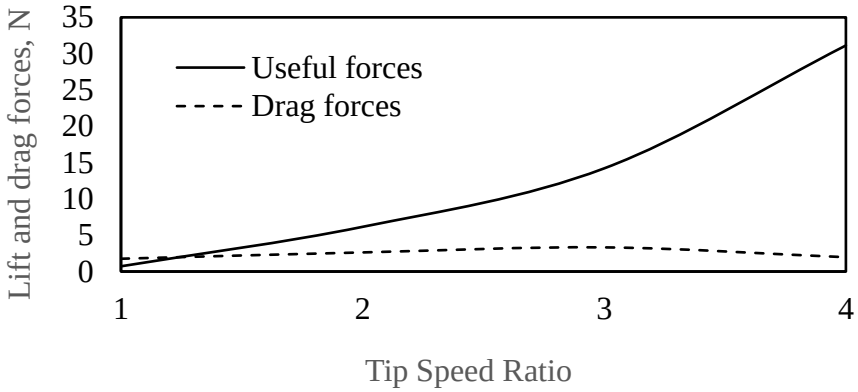

Figure 4.7: Lift and drag forces at TSR=1, 2, 3, 4 and pitch angle of 45^{o}

In Figures 4.8 and 4.9, the total average torque is -1.330 [N.m] at TSR=1, 4.511 [N.m] at TSR=2, 13.934 [N.m] at TSR=3, 37.324 [N.m] at TSR=4, and the corresponding average produced power is -24.407 [W] at TSR=1, 82.762 [W] at TSR=2, 255.613 [W] at TSR=3, and 684.708 [W] at TSR=4.

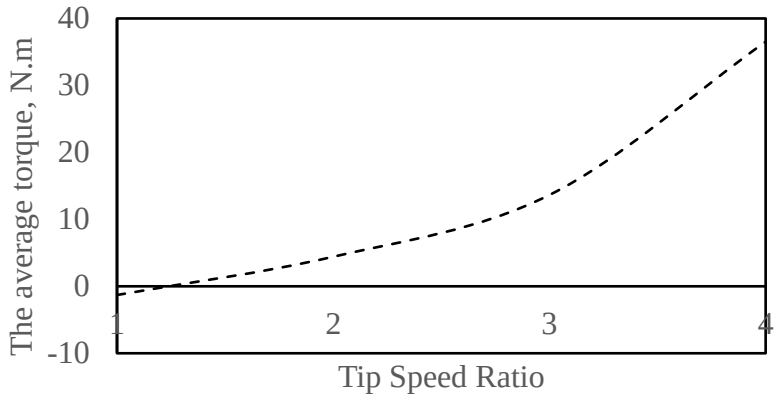

Figure 4.8: The total average torque at TSR=1, 2, 3, and 4 at pitch angle of 45º

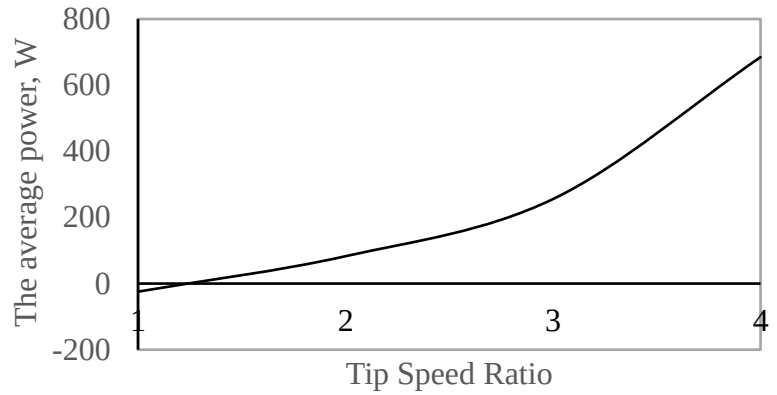

Figure 4.9: The total average produced power at TSR=1,2,3, and 4 at pitch angle of 45º

4.2.5 Results at TSR ranging from 1 to 4 and pitch angle fixed at 67.5º

The obtained results show that the produced torque and power are fluctuating according to the fixed pitch angles. The total average torque from the analyzed model of the three blades for this scenario is 0.017 [N.m] at TSR=1, 8.461 [N.m] at TSR=2, 21.431 [N.m] at TSR=3, 50.623 [N.m] at TSR=4, and the corresponding average produced

power is 0.306 [W] at TSR=1, 155.214 [W] at TSR=2, 393.145 [W] at TSR=3, and 928.687 [W] at TSR=4. The summary of the results is presented in Table A.4

, Appendix A.

The lift and drag forces used as well as the produced torque and power are presented in the following figures. The desired values of lift forces are higher than drag forces, as shown in Figure 4.10.

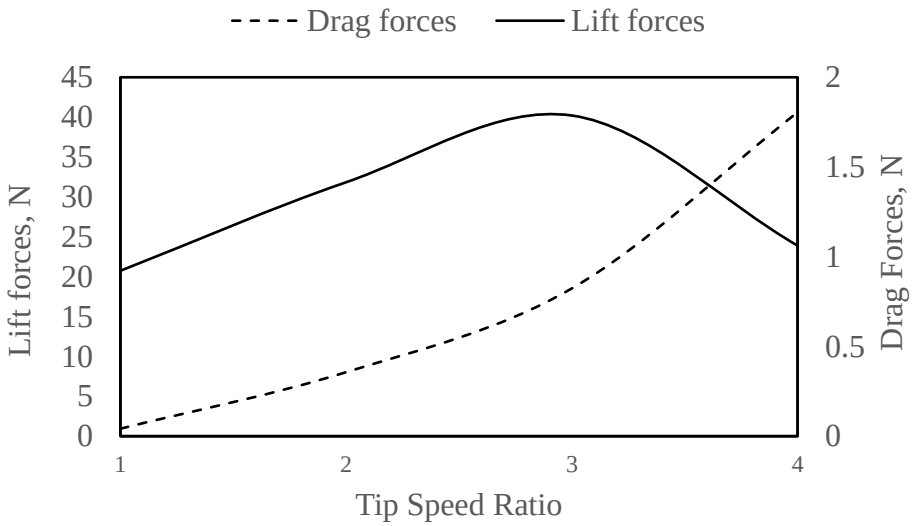

Figure 4.10: Lift and drag forces at TSR=1, 2, 3, 4 and pitch angle of 67.5^{o}

In Figures 4.11 and 4.12, the total average torque is 0.017 [N.m] at TSR=1, 8.461 [N.m] at TSR=2, 21.431 [N.m] at TSR=3, 50.623 [N.m] at TSR=4, and the corresponding average produced power is 0.306 [W] at TSR=1, 155.214 [W] at TSR=2, 393.145 [W] at TSR=3, and 928.687 [W] at TSR=4.

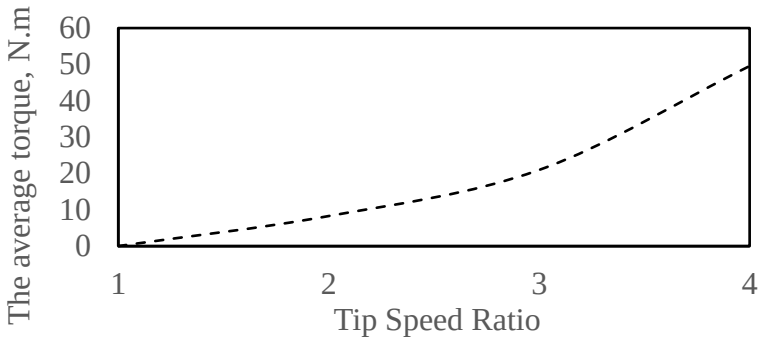

Figure 4.11: The total average torque at TSR=1, 2, 3, and 4 at pitch angle of 67.5^{o}

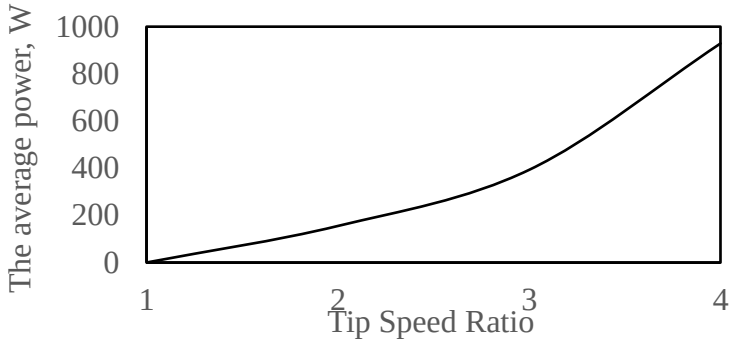

Figure 4.12: The total average produced power at TSR=1,2,3, and 4 at pitch angle of 67.5^{o}

4.2.6 Results at TSR ranging from 1 to 4 and pitch angle fixed at 90^{o}

The obtained results show that the produced torque and power are fluctuating according to the fixed pitch angles. The total average torque from the analyzed model of the three blades for this scenario is 1.361 [N.m] at TSR=1, 11.123 [N.m] at TSR=2, 25.666 [N.m] at TSR=3, 56.219 [N.m] at TSR=4, and the corresponding average

produced power is 24.972 [W] at TSR=1, 204.045 [W] at TSR=2, 470.846 [W] at TSR=3, and 1031.335 [W] at TSR=4. The summary of the results is presented in Table A.5, Appendix A. The results in this scenario are optimal values and it is highly recommended to use this tactic in practice.

The lift and drag forces used as well as the produced torque and power are presented in the following figures. The desired values of lift forces are higher than drag forces, as shown in Figure 4.13.

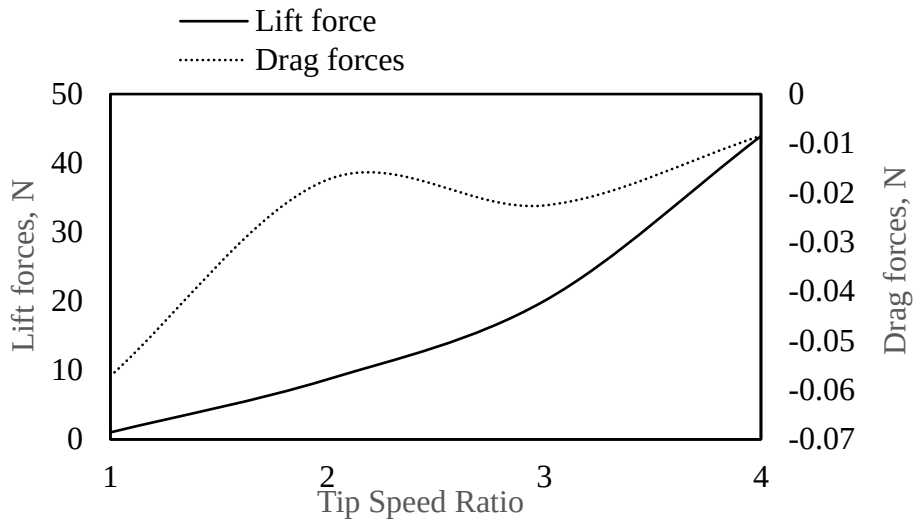

Figure 4.13: The average lift and drag forces at TSR=1, 2, 3, 4 and pitch angle of 90^{o}

In Figures 4.14 and 4.15, the total average torque is 1.361 [N.m] at TSR=1, 11.123 [N.m] at TSR=2, 25.666 [N.m] at TSR=3, 56.219 [N.m] at TSR=4, and the corresponding average produced power is 24.972 [W] at TSR=1, 204.045 [W] at TSR=2, 470.846 [W] at TSR=3, and 1031.335 [W] at TSR=4. The summary of the results is presented in Table

A.6. The results in this scenario are optimal values and it is highly recommended to use this tactic in practice.

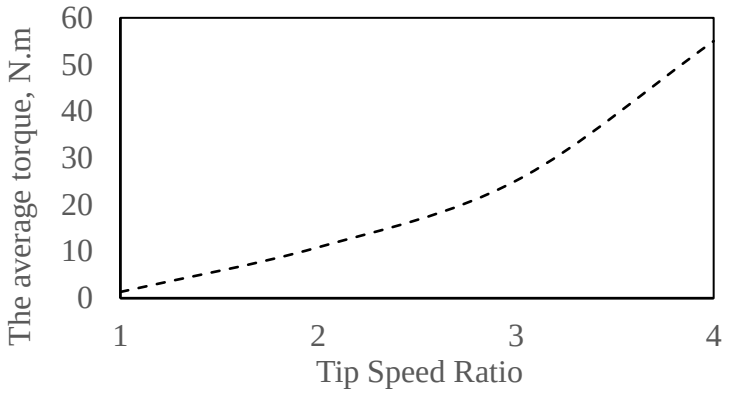

Figure 4.14: The total average torque at TSR=1, 2, 3, and 4 at pitch angle of 90°

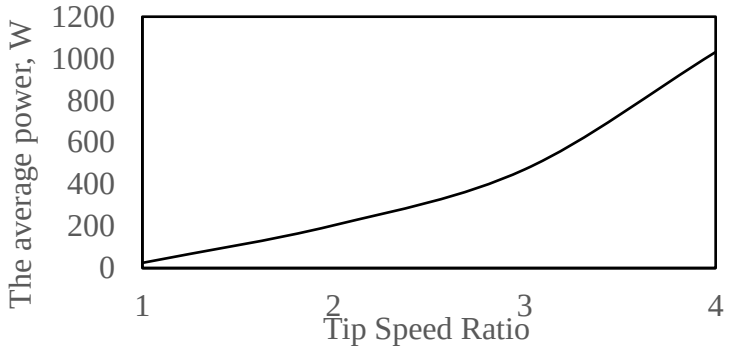

Figure 4.15: The total average produced power at TSR=1,2,3, and 4 at pitch angle of 90°

4.2.7 Results at TSR ranging from 1 to 4 and pitch angle fixed at 112.5º

The performance of the model in terms of increased power output changes as the blade pitch angles change, since this leads to a significant effect on the forces affecting the motion of the NASA0012 airfoils. The total average torque from the analyzed model of the three blades for this scenario is 2.499 [N.m] at TSR=1, 12.092 [N.m] at TSR=2, 25.996 [N.m] at TSR=3, 53.259 [N.m] at TSR=4, and the corresponding average produced power is 45.838 [W] at TSR=1, 221.823 [W] at TSR=2, 476.892 [W] at TSR=3, and 977.030 [W] at TSR=4.

The summary of the results is presented in Table A.7, Appendix A. The lift and drag forces used as well as the produced torque and power are presented in the following figures. The desired values of lift forces is higher than drag forces, as shown in Figure 4.16.

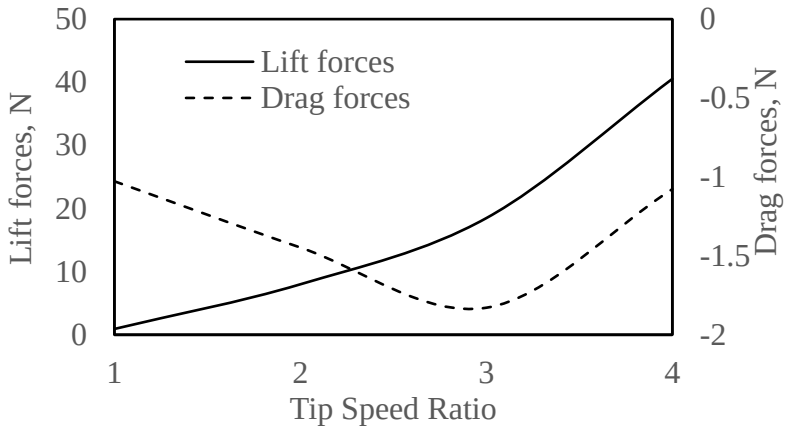

Figure 4.16: The average lift and drag forces at TSR=1, 2, 3, 4 and pitch angle of 112.5º

In Figures 4.17 and 4.18, the total average torque is 2.499 [N.m] at TSR=1, 12.092 [N.m] at TSR=2, 25.996 [N.m] at TSR=3, 53.259 [N.m] at TSR=4, and the corresponding average produced power is 45.838 [W] at TSR=1, 221.823 [W] at TSR=2, 476.892 [W] at TSR=3, and 977.030 [W] at TSR=4.

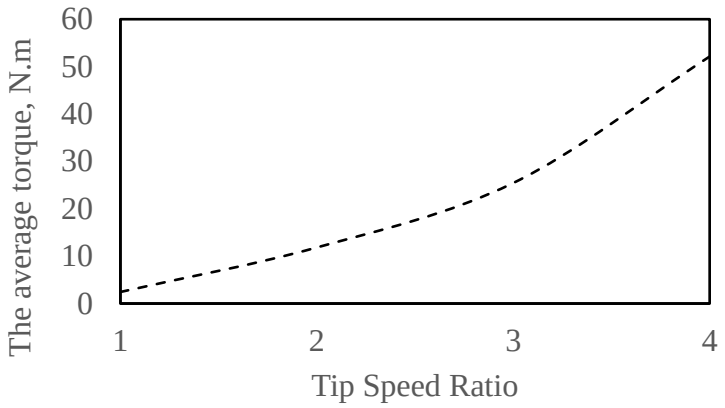

Figure 4.17: The total average torque at TSR=1, 2, 3, and 4 at pitch angle of 112.5º

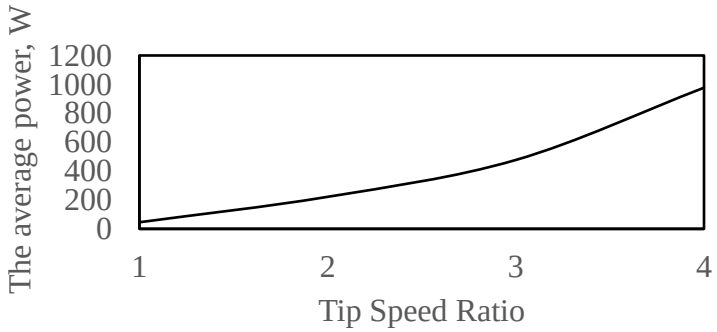

Figure 4.18: The total average produced power at TSR=1,2,3, and 4 at pitch angle of 112.5º

4.2.8 Results at TSR ranging from 1 to 4 and pitch angle fixed at 135º

Changing the blade pitch angles results in increasing or decreasing the torque and power of the model, which has an impact on the hurt and useful forces affecting the motion of the blades. The total average torque from the analyzed model of the three blades for this scenario is 3.256 [N.m] at TSR=1, 11.221 [N.m] at TSR=2, 22.369 [N.m] at TSR=3, 42.193 [N.m] at TSR=4, and the corresponding average produced power is 59.728 [W] at TSR=1, 205.844 [W] at TSR=2, 410.363 [W] at TSR=3, and 774.037 [W] at TSR=4. The summary of the results is presented in Table A.8, Appendix A.

The lift and drag forces used as well as the produced torque and power are presented in the following figures. The desired values of lift forces are higher than drag forces, as shown in Figure 4.19.

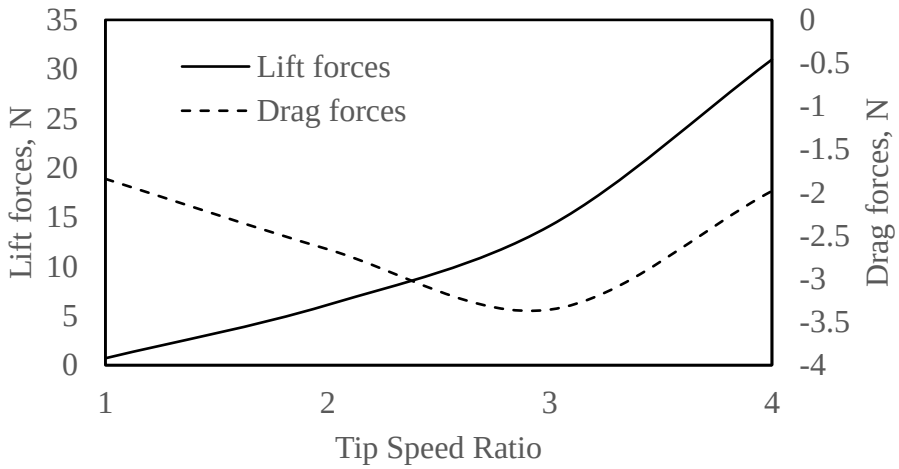

Figure 4.19: The average lift and drag forces at TSR=1, 2, 3, 4 and pitch angle of 135 º

In Figures 4.20 and 4.21, the total average torque is 3.256 [N.m] at TSR=1, 11.221 [N.m] at TSR=2, 22.369 [N.m] at TSR=3, 42.193 [N.m] at TSR=4, and the corresponding average produced power is 59.728 [W] at TSR=1, 205.844 [W] at TSR=2, 410.363 [W] at TSR=3, and 774.037 [W] at TSR=4.

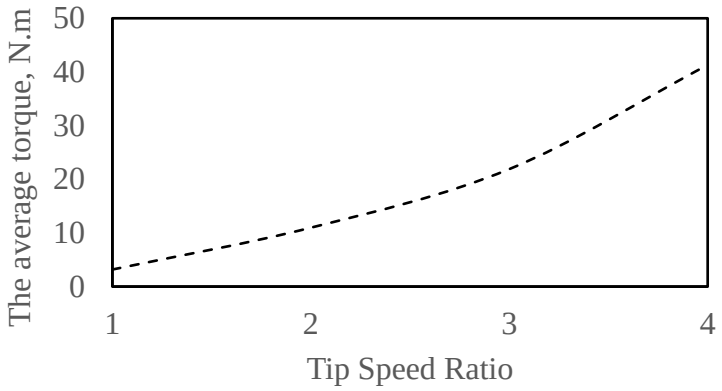

Figure 4.20: The total average torque at TSR=1, 2, 3, and 4 at pitch angle of 135^{o}

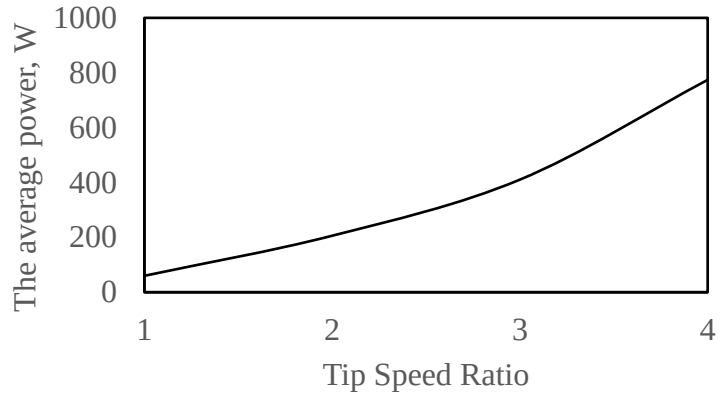

Figure 4.21: The total average produced power at TSR=1,2,3, and 4 at pitch angle of 135^{o}

4.2.9 Results at TSR ranging from 1 to 4 and pitch angle fixed at 157.5º

Changing the blade pitch angles results in increasing or decreasing the torque and power of the model, which has an impact on the hurt and useful forces affecting the motion of the blades. The total average torque from the analyzed model of the three blades for this scenario is 3.517 [N.m] at TSR=1, 8.642 [N.m] at TSR=2, 15.338 [N.m] at TSR=3, 24.707 [N.m] at TSR=4, and the corresponding average produced power is 64.528 [W] at TSR=1, 158.538 [W] at TSR=2, 281.382 [W] at TSR=3, and 453.247 [W] at TSR=4. The summary of the results is presented in Table A.9, Appendix A.

The lift and drag forces used as well as the produced torque and power are presented in the following figures. The desired values of lift forces are higher than drag forces, as shown in Figure 4.22.

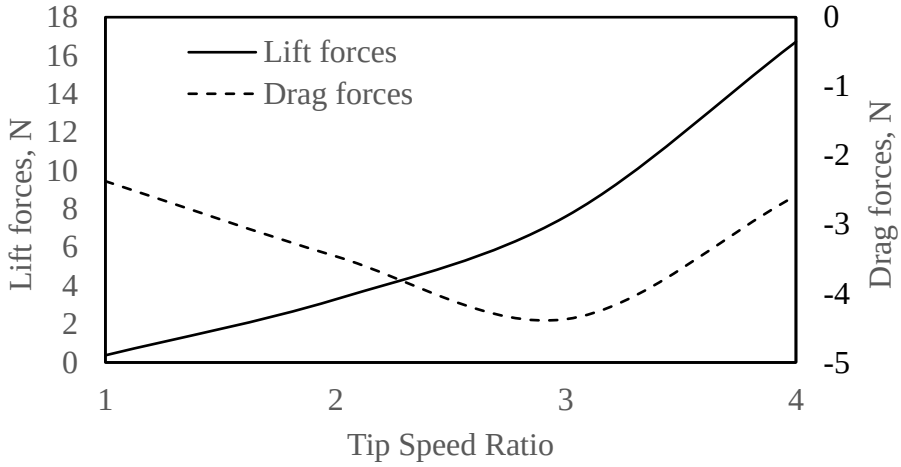

Figure 4.22: The average lift and drag forces at TSR=1, 2, 3, 4 and pitch angle of 157.5º

In Figures 4.23 and 4.24, the total average torque is 3.517 [N.m] at TSR=1, 8.642 [N.m] at TSR=2, 15.338 [N.m] at TSR=3, 24.707 [N.m] at TSR=4, and the corresponding average produced power is 64.528 [W] at TSR=1, 158.538 [W] at TSR=2, 281.382 [W] at TSR=3, and 453.247 [W] at TSR=4.

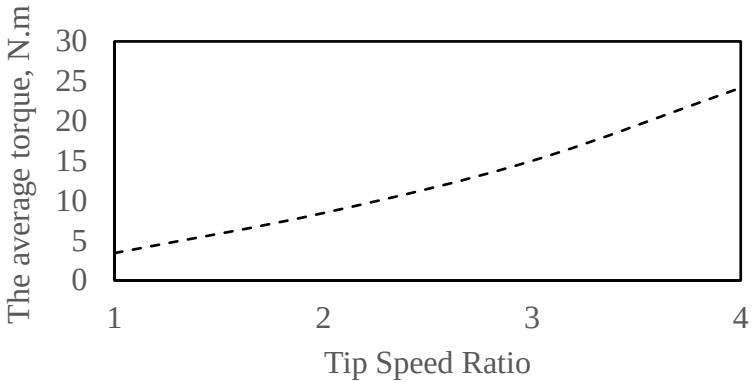

Figure 4.23: The total average torque at TSR=1, 2, 3, and 4 at pitch angle of 157.5°

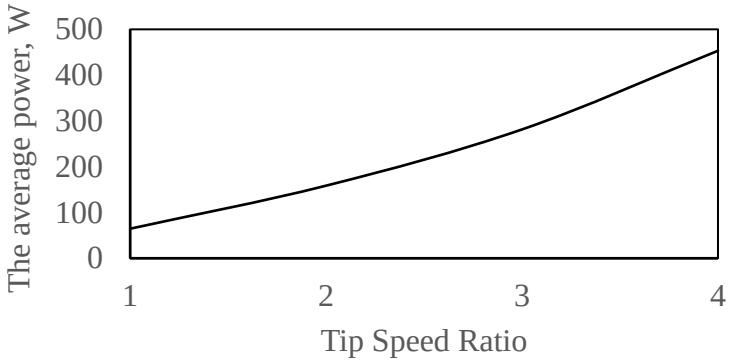

Figure 4.24: The total average produced power at TSR=1,2,3, and 4 at pitch angle of 157.5°

4.2.10 Results at TSR ranging from 1 to 4 and pitch angle fixed at 180º

Changing the blade pitch angles results in increasing or decreasing the torque and power of the model, which has an impact on the hurt and useful forces affecting the motion of the blades. The total average torque from the analyzed model of the three blades for this scenario is 3.244 [N.m] at TSR=1, 4.748 [N.m] at TSR=2, 5.973 [N.m] at TSR=3, 3.460 [N.m] at TSR=4, and the corresponding average produced power is 59.508 [W] at TSR=1, 87.105 [W] at TSR=2, 109.580 [W] at TSR=3, and 63.480 [W] at TSR=4. The summary of the results is presented in Table A.10, Appendix A.

The lift and drag forces used as well as the produced torque and power are presented in the following figures.

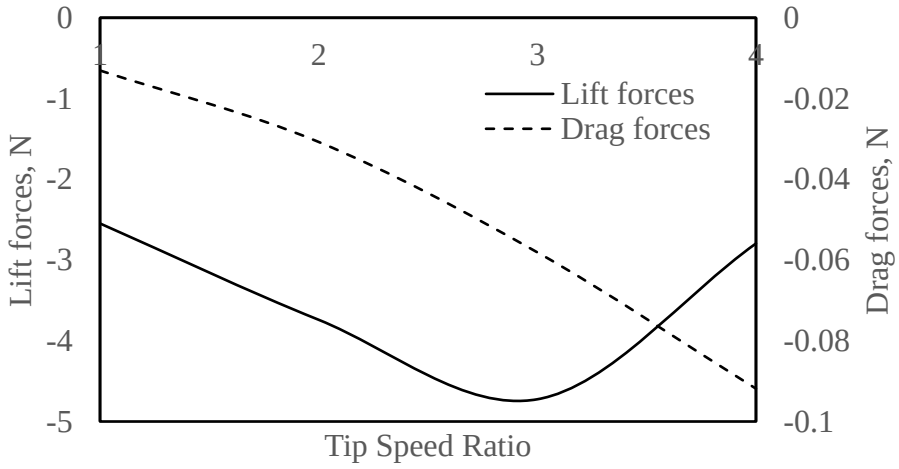

Figure 4.25: The average lift and drag forces at TSR=1, 2, 3, 4 and pitch angle of 180 º

In Figures 4.26 and 4.27, the total average torque is 3.244 [N.m] at TSR=1, 4.748 [N.m] at TSR=2, 5.973 [N.m] at TSR=3, 3.460 [N.m] at TSR=4, and the corresponding average produced power is 59.508 [W] at TSR=1, 87.105 [W] at TSR=2, 109.580 [W] at TSR=3, and 63.480 [W] at TSR=4.

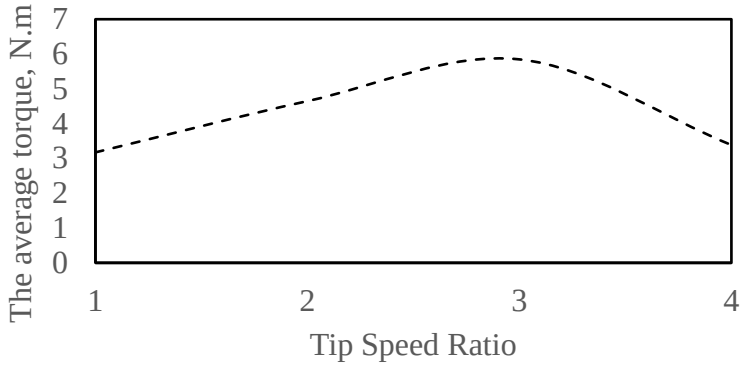

Figure 4.26: The total average torque at TSR=1, 2, 3, and 4 at pitch angle of 180^{o}

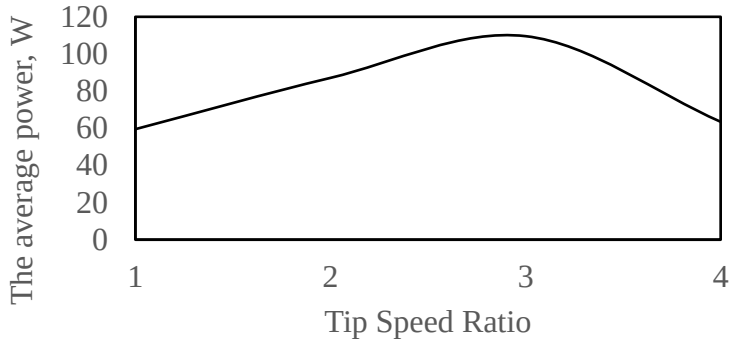

Figure 4.27: The total average produced power at TSR=1,2,3, and 4 at pitch angle of 180^{o}

4.2.11 The overall results at TSR ranging from 1 to 4 and pitch angle fixed at the range (0:22.5:180)º

It is evident that the torque and power extracted from the analyzed model can be positive or negative. The positive one occurs at the range (0:22.5:180), as well as the optimum values, which are at the fixed pitch angle of 90º. The negative torque and power are in the range (180:22.5:360), and they can be neglected since they seem to be in the opposite direction of the flow. In Figure 4.28, it can be seen that the maximum values of power for all values of tip speed ratios occur at a pitch angle of 90º. This blade pitch angle is the optimum value and the model therefore has to be analyzed and implemented at this angle, since it ensures the optimum values of torque and power.

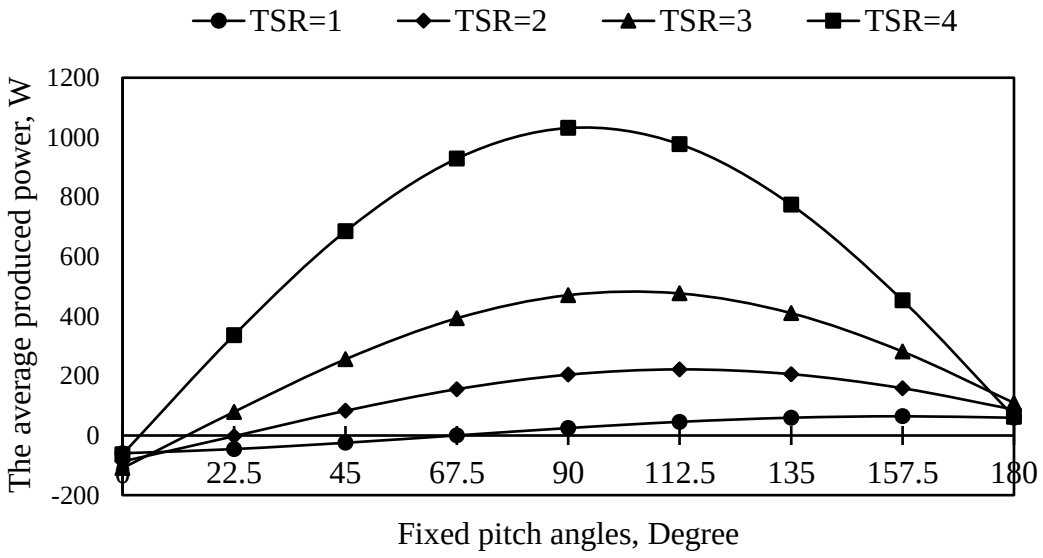

Figure 4.28: The total average produced power at TSR=1,2,3, and 4 at a pitch angle range of (0:22.5:180)

4.3 The overall results at TSR ranging from 1 to 4 are a function of the rotor position at the pitch angle range of (0:22.5:180)^{o}

In this analysis, many scenarios for an improved performance in terms of power output for a three straight-bladed VAWT model by introducing a variation in the blade pitch angles and taking them as functions of the rotor position are presented. The analysis is carried out over a wide range of blade angles by variations in pitch. The modifications are: 1- $\beta = 0.25\ \theta$. 2- $\beta = 0.5\ \theta$. 3- $\beta = \theta$. 4- $\beta = 22.5\ \theta$. 5- $\beta = 45\ \theta$. 6- $\beta = 67.5\ \theta$. 7- $\beta = 90\ \theta$. The results are presented in Table A.11. in Appendix A.

Obviously, the optimum value of the power occurs at $\beta = 22.5\ \theta$ of 736.135 W. However, this value is less than the optimum value obtained from the fixed pitch control technique. The following Figures 4.29 to 4.35 show the behavior of the power throughout the circle over a tip speed ratio range from 1 to 4. Figure 4.29 represents the results at TSR ranges from 1 to 4 and pitch angle of 0.25 of the rotor position. The optimum values of torque and power are 5.88 N.m and 107.88 W at TSR=4.

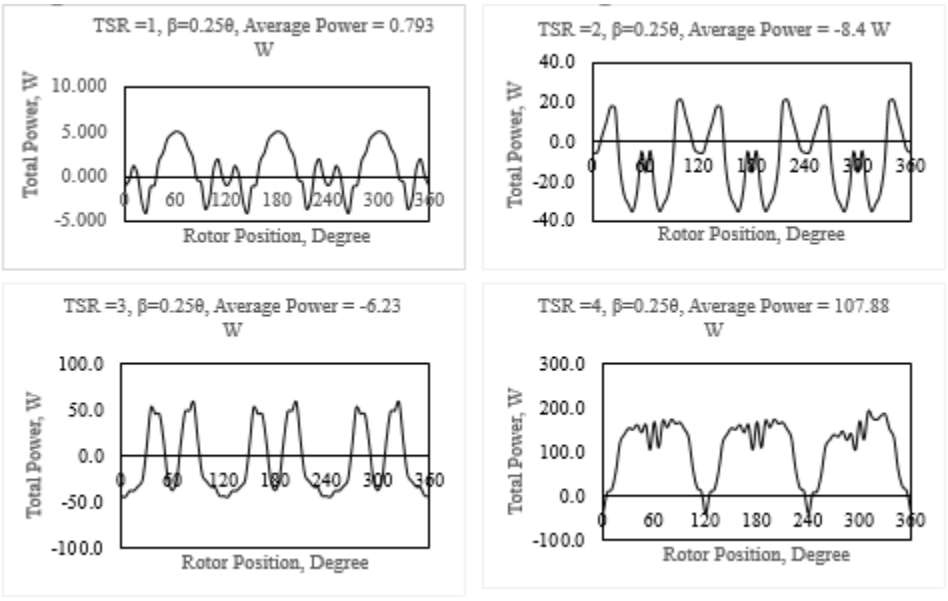

Figure 4.29: The total average produced power at TSR= 1, 2, 3, and 4 at pitch angle of 0.25 θ

Figure 4.30 represents the results at TSR ranges from 1 to 4 and pitch angle of 0.5 of the rotor position. The optimum values of torque and power are 6.3 N.m and 122.3 W at TSR=4.

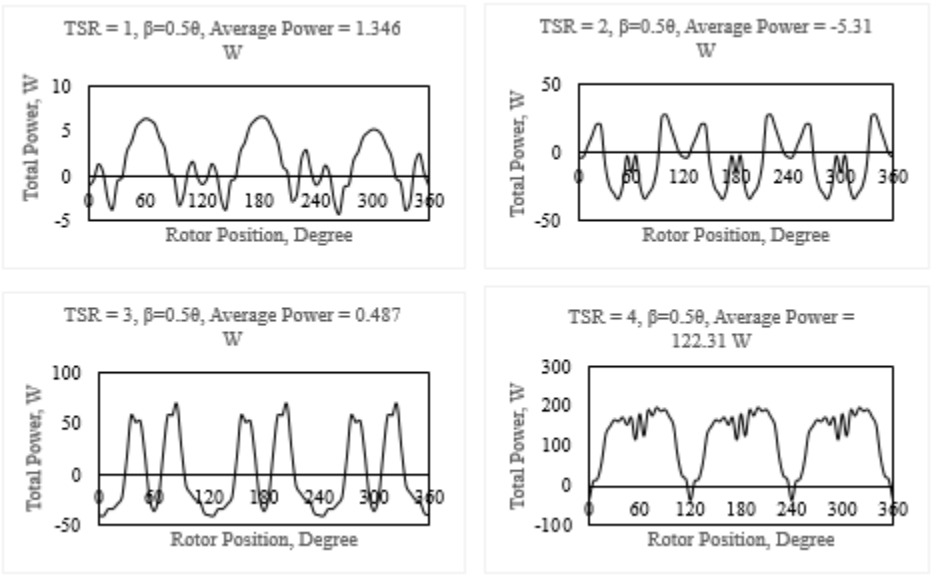

Figure 4.30: The total average produced power at TSR= 1, 2, 3, and 4 at pitch angle of 0.5 θ

Figure 4.31 represents the results at TSR ranges from 1 to 4 and pitch angle equal to the rotor position. The optimum values of torque and power are 7.35 N.m and 134.8 W at TSR=4.

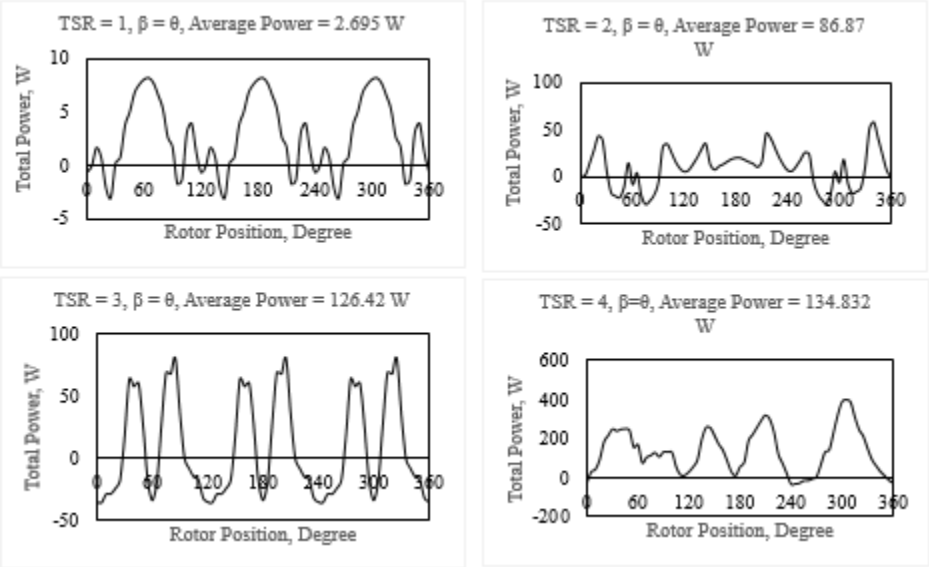

Figure 4.31: The total average produced power at TSR=1, 2, 3, and 4 at pitch angle equal to θ

Figure 4.32 represents the results at TSR ranges from 1 to 4 and pitch angle 22.5 of the rotor position. The optimum values of torque and power are 40.13 N.m and 736.1 W at TSR=4.

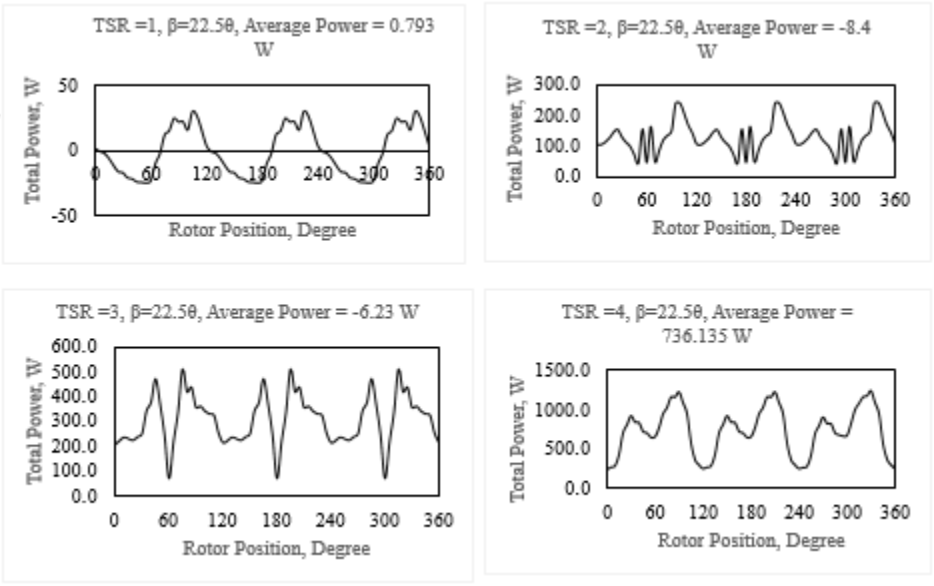

Figure 4.32: The total average produced power at TSR= 1, 2, 3, and 4 at pitch angle equal to 22.5 θ

Figure 4.33 represents the results at TSR ranges from 1 to 4 and pitch angle 45 times the rotor position. The optimum values of torque and power are 10.6 N.m and 140.4 W at TSR=4.

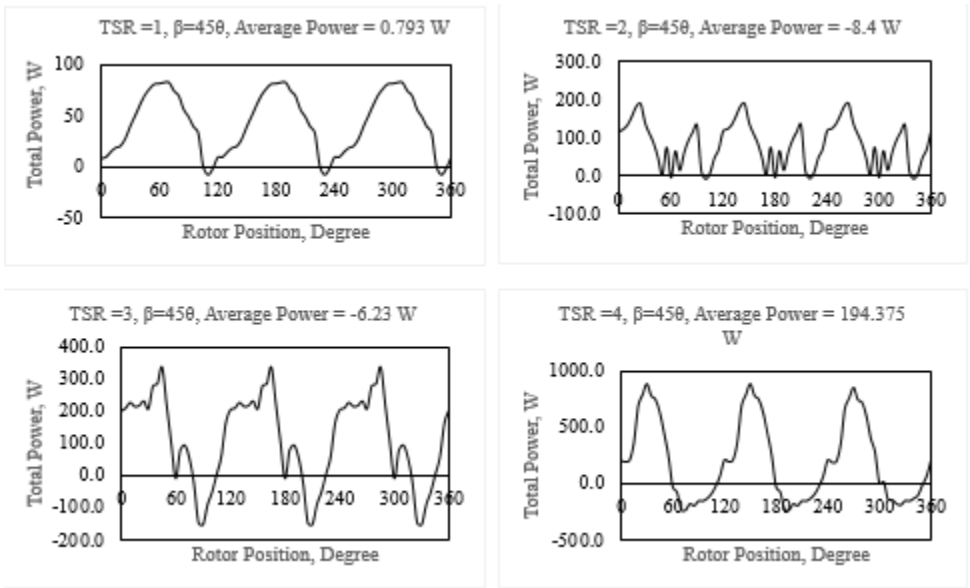

Figure 4.33: The total average produced power at TSR= 1, 2, 3, and 4 at pitch angle equal to 45 θ

Figure 4.34 represents the results at TSR ranges from 1 to 4 and pitch angle 67.5 times the rotor position. The optimum values of torque and power are 4.02 N.m and 73.9 W at TSR=4.

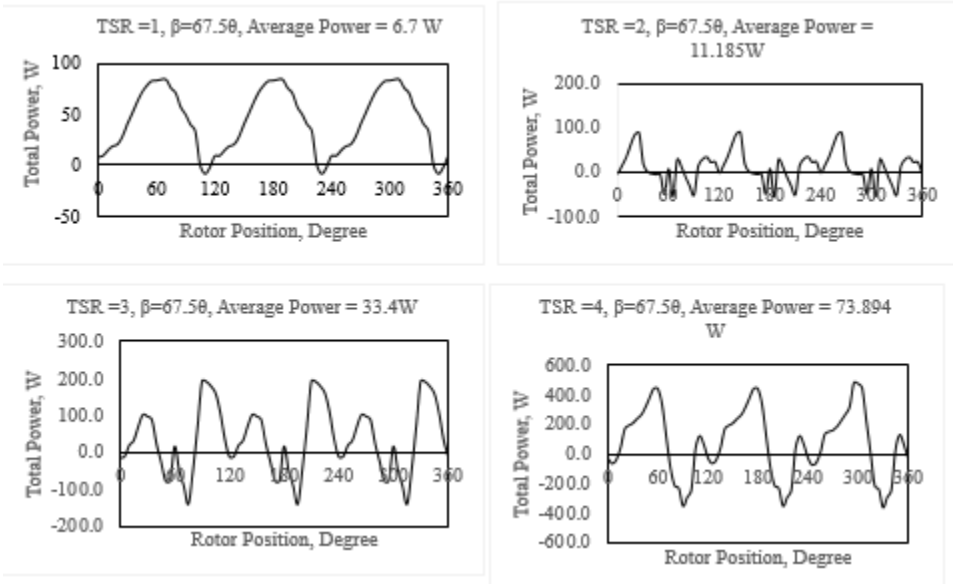

Figure 4.34: The total average produced power at TSR= 1, 2, 3, and 4 at pitch angle equal to 67.5 θ

Figure 4.35 represents the results at TSR ranges from 1 to 4 and pitch angle 90 times the rotor position. The optimum values of torque and power are 8.4 N.m and 154.1 W at TSR=4.

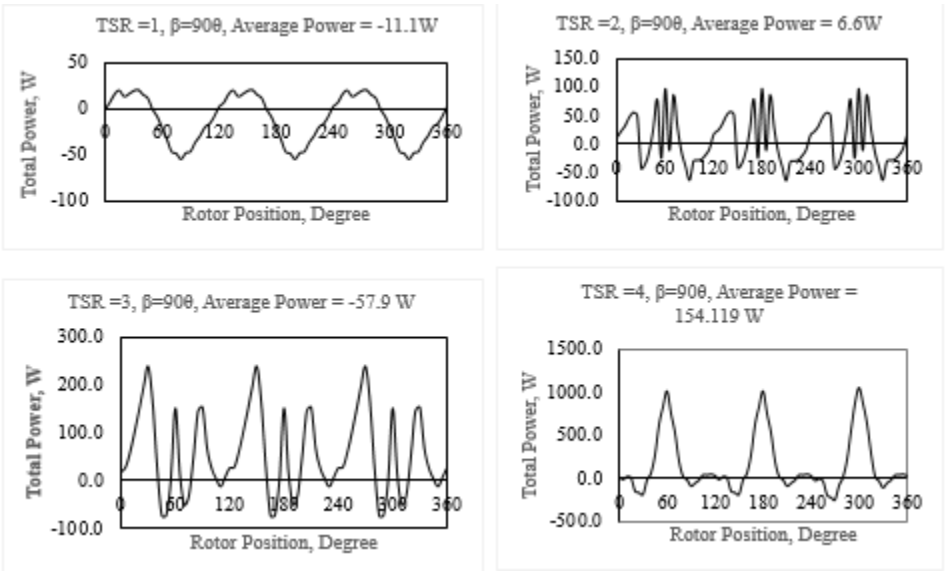

Figure 4.35: The total average produced power at TSR= 1, 2, 3, and 4 at pitch angle equal to 90 θ

Figure 4.36 shows the optimum produced power at the chosen values of blade pitch angles, - β = 0.25 θ. 2- β = 0.5 θ. 3- β = θ. 4- β = 22.5 θ. 5- β = 45 θ. 6- β = 67.5 θ. 7- β = 90 θ. One can see that the curve of produced power increases until it reaches its optimum value at blade pitch angle of 22.5 times the rotor position (β = 22.5 θ), and then decreases again. Hence, the value of β = 22.5 θ is the maximum value in this modification, since it provides us with the maximum torque and power at all values of tip speed ratios compared to other values of blade pitch angles.

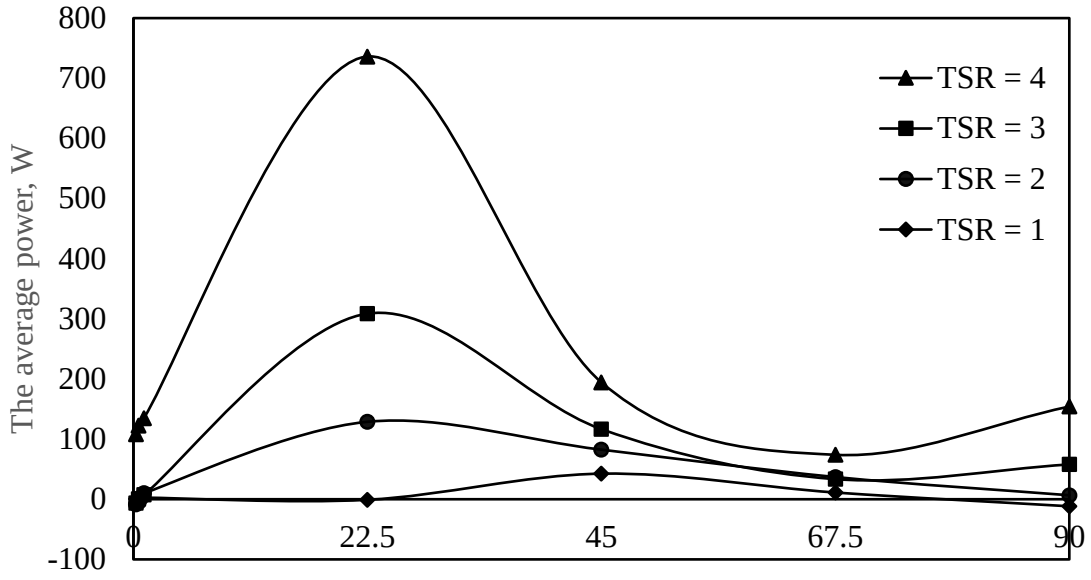

Figure 4.36: The total average produced power at TSR= 4 at pitch angles of 0, 22.5, 45, 67.5, and 90 times θ.

4.4 Results of annual energy production and capacity factor (Performance) of the model

The results collected from our analysis to find AEP and CF are based on equations 3.1 to 3.8. The results are Excel spreadsheet-based and are summarized in Table A.12, Appendix A. Even though the model has small power and dimensions, it has a satisfactory capacity factor of 19.524%, and a good annual energy production of 896.208 MWh, since it has been considered at the high wind speed of 6 m/s.

It is significant for us to study the factors affecting the annual energy productions (AEP) and capacity factors (CF). The most important factors are wind speed and hub

height. We will study the effects of hub height at constant wind speed, and the impacts of wind speeds at constant hub height.

4.4.1 The effects of the hub height at constant wind speed

The annual energy production and capacity factor increases considerably as hub height increases. The values of AEP and CF at H= 4 m are 896.208 kWh and 19.524 % respectively, while at H= 8 m the annual energy production and capacity factor are 1214.15 kWh and 26.45 % respectively, and so on**.** The results are shown in Table A.13, Appendix A.

4.4.2 The effects of wind speed at constant hub height

The effect of wind speeds on the performance and annual energy production are very important. However, it is necessary to avoid the high values of wind speed since they cause failure of the rotor blades. At a wind speed of 6 m/s the annual energy production and capacity factor were determined to be 896.208 kWh and 19.524 %; by increasing the wind speed to 10 m/s it was observed that the annual energy production and capacity factor increased to 4161.51 kWh and 0.9066%. The results are shown in Table A.14, Appendix A.

It is obvious from the previous results that the hub height and wind speed have their own impact on AEP and CF. The increase in AEP and CF as a result of changing hub height from 4 m to 6 m at the wind speed of 6 m/s was 16.278 % and the increase in AEP and CF as a result of increasing hub height from 6 m to 8 m was 11.834 %. In addition, the wind speeds played a major role in increasing the values of AEP and CF. For

example, the increasing of wind speeds from 6 to 8 m/s caused the AEP and CF to rise by 58.44 %, and by 48.18 % following an increase from 8 to 10 m/s.

4.5 Validation of the results for technique I with those of the same direction in the previous study

In order to validate the numerical results of the model presented in chapter four, a comparison between the model from the previous study and the current study was made for two values of blade pitch angles only, viz. 90 ^{o} and 107 ^{o}. The reason why we compared these two angles was that the previous study was carried out at only limited values of the blade pitch angles closest to the optimum value of 90^{o} . It is obvious from Figures 4.37 and 4.38 that the largest error between the current and previous studies did not exceed 15%. At the lowest values of the tip speed ratios, the errors were small and only began increasing when the tip speed ratios increased.

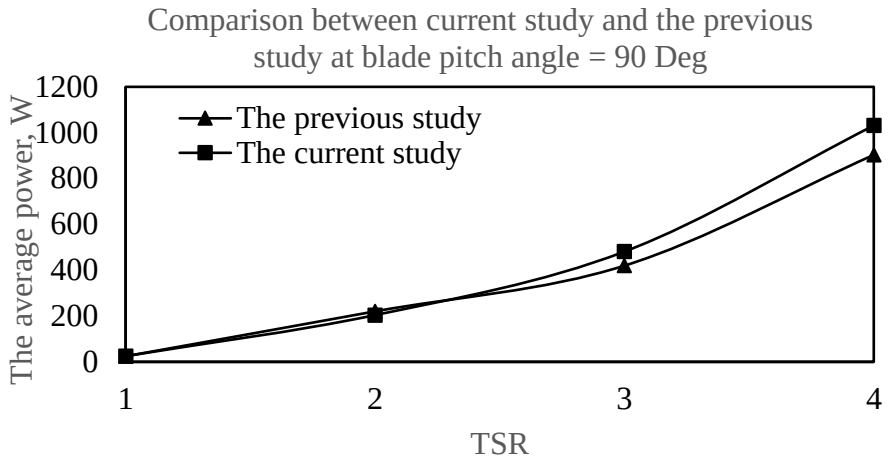

Figure 4.37: The comparison between the current study and the previous study at blade pitch angle of 90^{o}

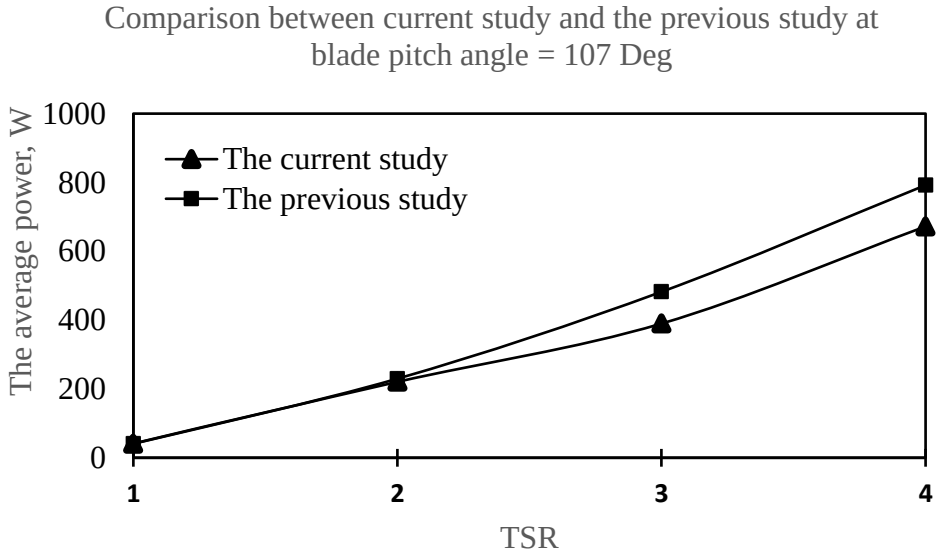

Figure 4.38: The comparison between the current study and the previous study at a blade pitch angle of 107

CHAPTER 5

CONCLUSIONS AND RECOMMENDATIONS

5.1 Conclusions

In this research, two techniques for an enhanced performance in terms of optimized power output for a straight – bladed vertical axis wind turbine by presenting a variation in the pitch angles of the blade are analyzed, along with the results. In addition, the annual energy production and capacity factor of the model are studied. These results can be summarized as follows:

1. Technique one examines the performance of the model when the blade pitch angles are kept fixed throughout the cycle of rotation. This method demonstrates the important increase in the power output at the optimum value of the blade pitch angle of 90o. This value of the blade pitch angle provides the maximum power of 1031.3 W compared to other fixed blade pitch angles, which is more than the optimum value of power obtained from the second technique.
2. Technique two investigates the behavior of torque and power when the variation of the blade pitch angles is introduced as functions of the rotor positions. A significant increase in power output was produced as a result of using this

modification. The optimum value of this technique is when the blade pitch angle equals 22.5 times the rotor position, with the maximum power of 736.135 W.

3. In addition to the above analysis, the investigation of performance in terms of studying the capacity factor and the annual energy production of the model is presented. This analysis results in an important increase of the values of the capacity factor and annual energy production. In addition, the effect of wind speed and hub height have played a major role in increasing the performance of the model.

5.2 Recommendations

Although the above modifications suggest an increase in the power output of a straight-bladed VAWT, the following points are recommended for future work:

1. Different types of the NASA airfoils should be used to investigate the best airfoil in terms of producing torque and power for the selected model.
2. An experimental model should be properly implemented to validate the obtained results to those of the experimental model.
3. Special designs of wind-direction sensors, blade pitch mechanism and power generation and transmission systems are required to achieve the desired performance.

APPENDICES

APPENDIX A: The total average power of the model at every position of the rotor of fixed pitch angles modification and tip speed ratio ranging from 1 to 4.

Table A 1: Results at TSR=1, 2, 3, 4 and pitch angles =0°.

Azimuth	Total Average Power (W)			
(θ)	TSR=1	TSR=2	TSR=3	TSR=4
0	-12.3	-98.1	-153.8	-127.3
5	-13.8	-99.8	-160.3	-77.2
10	-18.1	-95.5	-157.5	-75.8
15	-27.2	-95.7	-151.1	-74.1
20	-36.9	-96.3	-141.7	-72
25	-50.4	-96.8	-137.9	-71.1
30	-60.7	-100.2	-96.9	-70.5
35	-74.8	-100.5	-68	-50.3
40	-83.3	-92.1	-65.1	-29.7
45	-94.3	-79.5	-71	-28.7
50	-99.1	-58.7	-60.9	-26.6
55	-104.6	-50.3	-78.6	-91.4
60	-104.7	-48.8	-76.6	-41.8
65	-104.6	-50.3	-78.6	-91.4
70	-99.1	-58.9	-60.9	-26.6
75	-94.3	-79.6	-71	-28.7
80	-83.3	-92.3	-65.1	-29.7
85	-74.8	-100.8	-68	-50.3
90	-60.7	-100.6	-96.9	-70.5
95	-50.4	-96.9	-137.9	-71.1
100	-36.9	-96.5	-141.7	-72
105	-27.2	-96.1	-151.1	-74.1
110	-18.1	-96	-157.5	-75.8
115	-13.8	-100.4	-160.3	-77.2
120	-12.3	-98.8	-153.8	-127.3

Azimuth	Total Average Power (W)			
(θ)	TSR=1	TSR=2	TSR=3	TSR=4
125	-13.8	-100.5	-160.3	-77.2
130	-18.1	-96.3	-157.5	-75.8
135	-27.2	-96.6	-151.1	-74.1
140	-36.9	-97.1	-141.7	-72
145	-50.4	-97.5	-137.9	-71.1
150	-60.7	-101.1	-96.9	-70.5
155	-74.8	-101.1	-68	-50.3
160	-83.3	-92.5	-65.1	-29.7
165	-94.3	-79.5	-71	-28.7
170	-99.1	-58.6	-60.9	-26.6
175	-104.6	-50.2	-78.6	-91.4
180	-104.7	-48.5	-76.6	-41.8
185	-104.6	-50.2	-78.6	-91.4
190	-99.1	-58.6	-60.9	-26.6
195	-94.3	-79.5	-71	-28.7
200	-83.3	-92.5	-65.1	-29.7
205	-74.8	-101.1	-68	-50.3
210	-60.7	-101.1	-96.9	-70.5
215	-50.4	-97.5	-137.9	-71.1
220	-36.9	-97.1	-141.7	-72
225	-27.2	-96.6	-151.1	-74.1
230	-18.1	-96.3	-157.5	-75.8
235	-13.8	-100.5	-160.3	-77.2
240	-12.3	-98.8	-153.8	-127.3
245	-13.8	-100.4	-160.3	-77.1
250	-18.1	-96	-157.5	-75.6
255	-27.2	-96.1	-151.1	-73.8
260	-36.9	-96.5	-141.7	-71.5
265	-50.4	-96.9	-137.9	-70.2
270	-60.7	-100.6	-96.9	-69.9
275	-74.8	-100.8	-68	-49.8
280	-83.3	-92.3	-65.1	-28.7
285	-94.3	-79.6	-71	-28.5

Azimuth	Total Average Power (W)			
(θ)	TSR=1	TSR=2	TSR=3	TSR=4
290	-99.1	-58.9	-60.9	-26.5
295	-104.6	-50.3	-78.6	-90.4
300	-104.7	-48.8	-76.6	-40.6
305	-104.6	-50.3	-78.6	-90.8
310	-99.1	-58.7	-60.9	-25.8
315	-94.3	-79.5	-71	-28.1
320	-83.3	-92.1	-65.1	-29.7
325	-74.8	-100.5	-68	-29.7
330	-60.7	-100.2	-96.9	-50
335	-50.4	-96.8	-137.9	-71.1
340	-36.9	-96.3	-141.7	-72
345	-27.2	-95.7	-151.1	-74.1
350	-18.1	-95.5	-157.5	-75.8
355	-13.8	-99.8	-160.3	-77.2
360	-12.3	-98.1	-153.8	-127.3
Average	-59.5	-87	-109.3	-62.9

Table A 2: Results at TSR=1, 2, 3, 4 and pitch angle of 22.5°.

Azimuth	Total Average Power (W)			
(θ)	TSR=1	TSR=2	TSR=3	TSR=4
0	-8.8	-30.6	-27.2	9.8
5	-4.7	-13.2	-7.8	89.8
10	-3.8	1.6	35.2	127.7
15	-11.8	20.5	47.9	222
20	-28.4	33.9	62.2	371.8
25	-37.9	31.5	76.8	431.6
30	-45.6	-18.5	111.8	490.2
35	-56.4	-24.1	164.9	479.5
40	-65.7	-21.7	151.1	493.5

Azimuth	Total Average Power (W)			
(θ)	TSR=1	TSR=2	TSR=3	TSR=4
45	-75.3	-23.5	180	443.3
50	-82.7	-19	118.2	436.3
55	-88.6	34	49	338.5
60	-91.5	-10.8	-15.8	363
65	-88.6	34	49	338.5
70	-82.7	-19.1	118.2	436.3
75	-75.3	-23.7	180	443.3
80	-65.7	-22	151.1	493.5
85	-56.4	-24.4	164.9	479.5
90	-45.6	-18.9	111.8	490.2
95	-37.9	31.3	76.8	431.6
100	-28.4	33.6	62.2	371.8
105	-11.8	20.1	47.9	222
110	-3.8	1	35.2	127.7
115	-4.7	-13.9	-7.8	89.8
120	-8.8	-31.4	-27.2	9.8
125	-4.7	-14.1	-7.8	89.8
130	-3.8	0.7	35.2	127.7
135	-11.8	19.6	47.9	222
140	-28.4	33	62.2	371.8
145	-37.9	30.6	76.8	431.6
150	-45.6	-19.5	111.8	490.2
155	-56.4	-24.8	164.9	479.5
160	-65.7	-22.2	151.1	493.5
165	-75.3	-23.6	180	443.3
170	-82.7	-18.8	118.2	436.3
175	-88.6	34.2	49	338.5
180	-91.5	-10.5	-15.8	363
185	-88.6	34.2	49	338.5
190	-82.7	-18.8	118.2	436.3
195	-75.3	-23.6	180	443.3
200	-65.7	-22.2	151.1	493.5
205	-56.4	-24.8	164.9	479.5

Azimuth	Total Average Power (W)			
(θ)	TSR=1	TSR=2	TSR=3	TSR=4
210	-45.6	-19.5	111.8	490.2
215	-37.9	30.6	76.8	431.6
220	-28.4	33	62.2	371.8
225	-11.8	19.6	47.9	222
230	-3.8	0.7	35.2	127.7
235	-4.7	-14.1	-7.8	89.8
240	-8.8	-31.4	-27.2	9.8
245	-4.7	-13.9	-7.8	53.3
250	-3.8	1	35.2	91.8
255	-11.8	20.1	47.9	186.8
260	-28.4	33.6	62.2	337.7
265	-37.9	31.3	76.8	399
270	-45.6	-18.9	111.8	458.6
275	-56.4	-24.4	164.9	449
280	-65.7	-22	151.1	474.4
285	-75.3	-23.7	180	420.4
290	-82.7	-19.1	118.2	408.4
295	-88.6	34	49	355.4
300	-91.5	-10.8	-15.8	379
305	-88.6	34	49	384.3
310	-82.7	-19	118.2	480.5
315	-75.3	-23.5	180	484.5
320	-65.7	-21.7	151.1	493.5
325	-56.4	-24.1	164.9	497.7
330	-45.6	-18.5	111.8	507.3
335	-37.9	31.5	76.8	431.6
340	-28.4	33.9	62.2	371.7
345	-11.8	20.5	47.9	217.9
350	-3.8	1.6	35.2	131.9
355	-4.7	-13.2	-7.8	89.8
360	-8.8	-30.6	-27.2	9.8
Average	-45.4	-2.3	79.2	336.5

Table A 3: Results at TSR=1, 2, 3, 4 and Pitch angle of 45^{o}

Azimuth	Total Average Power (W)			
(θ)	TSR=1	TSR=2	TSR=3	TSR=4
0	-3.9	41.6	103.6	145.4
5	5.2	75.3	145.9	243.2
10	11.2	98.5	222.6	311.8
15	5.5	133.7	239.6	484.2
20	-15.5	159	256.7	758.9
25	-19.6	155	279.8	868.6
30	-23.7	66.1	303.5	976.3
35	-29.4	56	372.7	936.2
40	-38.2	51.9	344.3	941.7
45	-44.7	36	403.6	847.8
50	-53.7	23.6	279.3	832.8
55	-59.2	113.2	169.2	717
60	-64.4	28.7	47.3	712.5
65	-59.2	113.2	169.2	717
70	-53.7	23.5	279.3	832.8
75	-44.7	35.9	403.6	847.8
80	-38.2	51.7	344.3	941.7
85	-29.4	55.7	372.7	936.2
90	-23.7	65.7	303.5	976.3
95	-19.6	154.7	279.8	868.6
100	-15.5	158.7	256.7	758.9
105	5.5	133.2	239.6	484.2
110	11.2	97.9	222.6	311.8
115	5.2	74.6	145.9	243.2
120	-3.9	40.8	103.6	145.4
125	5.2	74.4	145.9	243.2
130	11.2	97.5	222.6	311.8
135	5.5	132.7	239.6	484.2
140	-15.5	158	256.7	758.9
145	-19.6	154.1	279.8	868.6
150	-23.7	65.1	303.5	976.3

Azimuth	Total Average Power (W)			
(θ)	TSR=1	TSR=2	TSR=3	TSR=4
155	-29.4	55.3	372.7	936.2
160	-38.2	51.5	344.3	941.7
165	-44.7	36	403.6	847.8
170	-53.7	23.8	279.3	832.8
175	-59.2	113.3	169.2	717
180	-64.4	29	47.3	712.5
185	-59.2	113.3	169.2	717
190	-53.7	23.8	279.3	832.8
195	-44.7	36	403.6	847.8
200	-38.2	51.5	344.3	941.7
205	-29.4	55.3	372.7	936.2
210	-23.7	65.1	303.5	976.3
215	-19.6	154.1	279.8	868.6
220	-15.5	158	256.7	758.9
225	5.5	132.7	239.6	484.2
230	11.2	97.5	222.6	311.8
235	5.2	74.4	145.9	243.2
240	-3.9	40.8	103.6	145.4
245	5.2	74.6	145.9	175.7
250	11.2	97.9	222.6	245.2
255	5.5	133.2	239.6	418.9
260	-15.5	158.7	256.7	695.5
265	-19.6	154.7	279.8	807.4
270	-23.7	65.7	303.5	917.2
275	-29.4	55.7	372.7	879.5
280	-38.2	51.7	344.3	905.3
285	-44.7	35.9	403.6	805.4
290	-53.7	23.5	279.3	781.2
295	-59.2	113.2	169.2	747.2
300	-64.4	28.7	47.3	740.9
305	-59.2	113.2	169.2	801
310	-53.7	23.6	279.3	913.6
315	-44.7	36	403.6	923.2

Azimuth	Total Average Power (W)			
(θ)	TSR=1	TSR=2	TSR=3	TSR=4
320	-38.2	51.9	344.3	941.7
325	-29.4	56	372.7	949.3
330	-23.7	66.1	303.5	987.5
335	-19.6	155	279.8	868.6
340	-15.5	159	256.7	758.9
345	5.5	133.7	239.6	476.7
350	11.2	98.5	222.6	319.6
355	5.2	75.3	145.9	243.2
360	-3.9	41.6	103.6	145.4
Average	-24.4	82.8	255.6	684.7

Table A 4: Results at TSR=1, 2, 3, 4 and Pitch angle of 67.5^{o}.

Azimuth	Total Average Power (W)			
(θ)	TSR=1	TSR=2	TSR=3	TSR=4
0	1.6	107.5	218.5	258.9
5	14.2	152.4	277.4	359.5
10	24.4	180.4	376.1	448.5
15	22	226.5	394.9	672.8
20	-0.3	259.8	412.1	1030.6
25	1.7	254.9	440.2	1173.4
30	1.9	140.6	449	1313.8
35	2.1	127.6	523.7	1250.5
40	-4.8	117.7	485.1	1246.5
45	-7.4	90.1	565.8	1123.3
50	-16.5	62.7	397.9	1102.6
55	-20.8	175.1	263.6	986.3
60	-27.5	63.9	103.3	953.6
65	-20.8	175.1	263.6	986.3
70	-16.5	62.6	397.9	1102.6
75	-7.4	90	565.8	1123.3

Azimuth	Total Average Power (W)			
(θ)	TSR=1	TSR=2	TSR=3	TSR=4
80	-4.8	117.5	485.1	1246.5
85	2.1	127.3	523.7	1250.5
90	1.9	140.3	449	1313.8
95	1.7	254.6	440.2	1173.4
100	-0.3	259.6	412.1	1030.6
105	22	226.1	394.9	672.8
110	24.4	179.9	376.1	448.5
115	14.2	151.9	277.4	359.5
120	1.6	106.8	218.5	258.9
125	14.2	151.7	277.4	359.5
130	24.4	179.6	376.1	448.5
135	22	225.7	394.9	672.8
140	-0.3	259.1	412.1	1030.6
145	1.7	254.1	440.2	1173.4
150	1.9	139.8	449	1313.8
155	2.1	127	523.7	1250.5
160	-4.8	117.4	485.1	1246.5
165	-7.4	90	565.8	1123.3
170	-16.5	62.8	397.9	1102.6
175	-20.8	175.3	263.6	986.3
180	-27.5	64.2	103.3	953.6
185	-20.8	175.3	263.6	986.3
190	-16.5	62.8	397.9	1102.6
195	-7.4	90	565.8	1123.3
200	-4.8	117.4	485.1	1246.5
205	2.1	127	523.7	1250.5
210	1.9	139.8	449	1313.8
215	1.7	254.1	440.2	1173.4
220	-0.3	259.1	412.1	1030.6
225	22	225.7	394.9	672.8
230	24.4	179.6	376.1	448.5
235	14.2	151.7	277.4	359.5
240	1.6	106.8	218.5	258.9

Azimuth	Total Average Power (W)			
(θ)	TSR=1	TSR=2	TSR=3	TSR=4
245	14.2	151.9	277.4	271.3
250	24.4	179.9	376.1	361.3
255	22	226.1	394.9	587.3
260	-0.3	259.6	412.1	947.4
265	1.7	254.6	440.2	1093
270	1.9	140.3	449	1236.2
275	2.1	127.3	523.7	1176.2
280	-4.8	117.5	485.1	1198.5
285	-7.4	90	565.8	1067.8
290	-16.5	62.6	397.9	1035
295	-20.8	175.1	263.6	1025.3
300	-27.5	63.9	103.3	990.1
305	-20.8	175.1	263.6	1095.7
310	-16.5	62.7	397.9	1207.8
315	-7.4	90.1	565.8	1221.5
320	-4.8	117.7	485.1	1246.5
325	2.1	127.6	523.7	1256.5
330	1.9	140.6	449	1317.3
335	1.7	254.9	440.2	1173.4
340	-0.3	259.8	412.1	1030.6
345	22	226.5	394.9	663
350	24.4	180.4	376.1	458.6
355	14.2	152.4	277.4	359.5
360	1.6	107.5	218.5	258.9
Average	0.3	155.2	393.1	928.7

Table A 5: Results at TSR=1, 2, 3, 4 and pitch angle of 90^{o}.

Azimuth	Total Average Power (W)			
(θ)	TSR=1	TSR=2	TSR=3	TSR=4
0	6.8	157	300.2	332.9

Azimuth	Total Average Power (W)			
(θ)	TSR=1	TSR=2	TSR=3	TSR=4
5	21.1	206.3	366.7	421.1
10	33.9	234.8	472.4	516.9
15	35.1	284.8	490	759
20	14.9	321.2	504.8	1145.5
25	22.8	316	533.7	1299.7
30	27.2	193.7	526.2	1451.4
35	33.3	179.7	595.1	1374.5
40	29.3	165.6	552.1	1361.7
45	31	130.4	641.9	1227.9
50	23.2	92.2	456	1204.5
55	20.8	210.4	317.9	1105.6
60	13.6	89.4	143.6	1049.5
65	20.8	210.4	317.9	1105.6
70	23.2	92.1	456	1204.5
75	31	130.4	641.9	1227.9
80	29.3	165.5	552.1	1361.7
85	33.3	179.6	595.1	1374.5
90	27.2	193.5	526.2	1451.4
95	22.8	315.8	533.7	1299.7
100	14.9	320.9	504.8	1145.5
105	35.1	284.5	490	759
110	33.9	234.5	472.4	516.9
115	21.1	206	366.7	421.1
120	6.8	156.6	300.2	332.9
125	21.1	205.8	366.7	421.1
130	33.9	234.3	472.4	516.9
135	35.1	284.3	490	759
140	14.9	320.6	504.8	1145.5
145	22.8	315.5	533.7	1299.7
150	27.2	193.2	526.2	1451.4
155	33.3	179.4	595.1	1374.5
160	29.3	165.4	552.1	1361.7
165	31	130.4	641.9	1227.9

Azimuth	Total Average Power (W)			
(θ)	TSR=1	TSR=2	TSR=3	TSR=4
170	23.2	92.2	456	1204.5
175	20.8	210.5	317.9	1105.6
180	13.6	89.5	143.6	1049.5
185	20.8	210.5	317.9	1105.6
190	23.2	92.2	456	1204.5
195	31	130.4	641.9	1227.9
200	29.3	165.4	552.1	1361.7
205	33.3	179.4	595.1	1374.5
210	27.2	193.2	526.2	1451.4
215	22.8	315.5	533.7	1299.7
220	14.9	320.6	504.8	1145.5
225	35.1	284.3	490	759
230	33.9	234.3	472.4	516.9
235	21.1	205.8	366.7	421.1
240	6.8	156.6	300.2	332.9
245	21.1	206	366.7	325.6
250	33.9	234.5	472.4	422.5
255	35.1	284.5	490	666.3
260	14.9	320.9	504.8	1055.2
265	22.8	315.8	533.7	1212.2
270	27.2	193.5	526.2	1367.1
275	33.3	179.6	595.1	1293.8
280	29.3	165.5	552.1	1309.3
285	31	130.4	641.9	1167.8
290	23.2	92.1	456	1131.4
295	20.8	210.4	317.9	1147.4
300	13.6	89.4	143.6	1088.6
305	20.8	210.4	317.9	1223.7
310	23.2	92.2	456	1318.1
315	31	130.4	641.9	1333.9
320	29.3	165.6	552.1	1361.7
325	33.3	179.7	595.1	1372.4
330	27.2	193.7	526.2	1446.7

Azimuth	Total Average Power (W)			
(θ)	TSR=1	TSR=2	TSR=3	TSR=4
335	22.8	316	533.7	1299.7
340	14.9	321.2	504.8	1145.5
345	35.1	284.8	490	748.4
350	33.9	234.8	472.4	527.8
355	21.1	206.3	366.7	421.1
360	6.8	157	300.2	333
Average	25	204	470.8	1031.3

Table A 6: Results at TSR=1, 2, 3, 4 and pitch angle of 112.5^{o}.

Azimuth	Total Average Power (W)			
(θ)	TSR=1	TSR=2	TSR=3	TSR=4
0	11	182.6	336.3	356.4
5	24.7	228.8	400.1	418.7
10	38.3	253.5	496.8	506.6
15	42.8	299.8	510.6	729.6
20	27.9	333.6	520.7	1086
25	40.3	329	545.9	1228.1
30	48.3	217.3	523.3	1368.1
35	59.4	204.5	575.9	1289.3
40	58.9	188.2	535	1269.6
45	64.8	150.9	620.3	1145.6
50	59.4	107.6	444.6	1123.2
55	59.2	213.6	323.9	1056.6
60	52.6	101.3	162	985.8
65	59.2	213.7	323.9	1056.6
70	59.4	107.7	444.6	1123.2
75	64.8	151	620.3	1145.6
80	58.9	188.2	535	1269.6
85	59.4	204.5	575.9	1289.3
90	48.3	217.3	523.3	1368.1
95	40.3	328.8	545.9	1228.1
100	27.9	333.5	520.7	1086

Azimuth	Total Average Power (W)			
(θ)	TSR=1	TSR=2	TSR=3	TSR=4
105	42.8	299.7	510.6	729.6
110	38.3	253.4	496.8	506.6
115	24.7	228.7	400.1	418.7
120	11	182.5	336.3	356.4
125	24.7	228.7	400.1	418.7
130	38.3	253.4	496.8	506.6
135	42.8	299.6	510.6	729.6
140	27.9	333.4	520.7	1086
145	40.3	328.8	545.9	1228.1
150	48.3	217.2	523.3	1368.1
155	59.4	204.5	575.9	1289.3
160	58.9	188.2	535	1269.6
165	64.8	150.9	620.3	1145.6
170	59.4	107.6	444.6	1123.2
175	59.2	213.7	323.9	1056.6
180	52.6	101.3	162	985.8
185	59.2	213.7	323.9	1056.6
190	59.4	107.6	444.6	1123.2
195	64.8	150.9	620.3	1145.6
200	58.9	188.2	535	1269.6
205	59.4	204.5	575.9	1289.3
210	48.3	217.2	523.3	1368.1
215	40.3	328.8	545.9	1228.1
220	27.9	333.4	520.7	1086
225	42.8	299.6	510.6	729.6
230	38.3	253.4	496.8	506.6
235	24.7	228.7	400.1	418.7
240	11	182.5	336.3	356.4
245	24.7	228.7	400.1	330.4
250	38.3	253.4	496.8	419.3
255	42.8	299.7	510.6	643.9
260	27.9	333.5	520.7	1002.3
265	40.3	328.8	545.9	1146.9

Azimuth	Total Average Power (W)			
(θ)	TSR=1	TSR=2	TSR=3	TSR=4
270	48.3	217.3	523.3	1290
275	59.4	204.5	575.9	1214.6
280	58.9	188.2	535	1220.8
285	64.8	151	620.3	1089.9
290	59.4	107.7	444.6	1055.5
295	59.2	213.7	323.9	1094.8
300	52.6	101.3	162	1021.4
305	59.2	213.6	323.9	1165.5
310	59.4	107.6	444.6	1227.9
315	64.8	150.9	620.3	1243.3
320	58.9	188.2	535	1269.6
325	59.4	204.5	575.9	1279.5
330	48.3	217.3	523.3	1356
335	40.3	329	545.9	1228.1
340	27.9	333.6	520.7	1086
345	42.8	299.8	510.6	719.9
350	38.3	253.5	496.8	516.7
355	24.7	228.8	400.1	418.7
360	11	182.6	336.3	356.4
Average	45.8	221.8	476.9	977

Table A 7: Results at TSR=1, 2, 3, 4 and pitch angle of 135^{o}.

Azimuth	Total Average Power (W)			
(θ)	TSR=1	TSR=2	TSR=3	TSR=4
0	13.5	180.4	321.1	325.5
5	24.6	216.5	372.7	352.5
10	36.8	233.7	445.6	419.3
15	44.1	269.2	453.5	589.3
20	36.7	295.3	457.3	861.3
25	51.8	291.9	475	969.7

Azimuth	Total Average Power (W)			
(θ)	TSR=1	TSR=2	TSR=3	TSR=4
30	62.1	207.8	440.7	1076.6
35	76.5	198.2	469	1007.9
40	79.6	182.3	436.6	984.3
45	88.6	148.5	504.3	888.9
50	86.5	106.7	365.6	870.9
55	88.6	184.4	280.5	846.8
60	83.6	97.7	155.8	772
65	88.6	184.4	280.5	846.8
70	86.5	106.8	365.6	870.9
75	88.6	148.5	504.3	888.9
80	79.6	182.4	436.6	984.3
85	76.5	198.3	469	1007.9
90	62.1	208	440.7	1076.6
95	51.8	291.9	475	969.7
100	36.7	295.3	457.3	861.3
105	44.1	269.2	453.5	589.3
110	36.8	233.8	445.6	419.3
115	24.6	216.7	372.7	352.5
120	13.5	180.6	321.1	325.5
125	24.6	216.7	372.7	352.5
130	36.8	233.9	445.6	419.3
135	44.1	269.4	453.5	589.3
140	36.7	295.5	457.3	861.3
145	51.8	292.1	475	969.7
150	62.1	208.2	440.7	1076.6
155	76.5	198.4	469	1007.9
160	79.6	182.4	436.6	984.3
165	88.6	148.5	504.3	888.9
170	86.5	106.7	365.6	870.9
175	88.6	184.4	280.5	846.8
180	83.6	97.6	155.8	772
185	88.6	184.4	280.5	846.8
190	86.5	106.7	365.6	870.9

Azimuth	Total Average Power (W)			
(θ)	TSR=1	TSR=2	TSR=3	TSR=4
195	88.6	148.5	504.3	888.9
200	79.6	182.4	436.6	984.3
205	76.5	198.4	469	1007.9
210	62.1	208.2	440.7	1076.6
215	51.8	292.1	475	969.7
220	36.7	295.5	457.3	861.3
225	44.1	269.4	453.5	589.3
230	36.8	233.9	445.6	419.3
235	24.6	216.7	372.7	352.5
240	13.5	180.6	321.1	325.5
245	24.6	216.7	372.7	284.9
250	36.8	233.8	445.6	352.3
255	44.1	269.2	453.5	523.5
260	36.7	295.3	457.3	797
265	51.8	291.9	475	907.1
270	62.1	208	440.7	1016.5
275	76.5	198.3	469	950.5
280	79.6	182.4	436.6	946.5
285	88.6	148.5	504.3	846.3
290	86.5	106.8	365.6	819.1
295	88.6	184.4	280.5	875.6
300	83.6	97.7	155.8	798.8
305	88.6	184.4	280.5	929.9
310	86.5	106.7	365.6	950.7
315	88.6	148.5	504.3	963.5
320	79.6	182.3	436.6	984.3
325	76.5	198.2	469	991.9
330	62.1	207.8	440.7	1058.8
335	51.8	291.9	475	969.7
340	36.7	295.3	457.3	861.3
345	44.1	269.2	453.5	581.8
350	36.8	233.7	445.6	426.9
355	24.6	216.5	372.7	352.5

Azimuth	Total Average Power (W)			
(θ)	TSR=1	TSR=2	TSR=3	TSR=4
360	13.5	180.4	321.1	325.5
Average	59.7	205.8	410.4	774

Table A 8: Results at TSR=1, 2, 3, 4 and pitch angle of 157.5°.

Azimuth	Total Average Power (W)			
(θ)	TSR=1	TSR=2	TSR=3	TSR=4
0	14	150.8	257.1	245.2
5	20.8	171.2	288.6	232.7
10	29.7	178.2	326.5	268.1
15	38.6	197.6	327.3	359.2
20	39.8	212	324.3	505.4
25	55.3	210.5	331.9	563.7
30	66.4	166.8	291.1	621.2
35	81.9	161.7	290.8	573.1
40	88.1	148.5	271.7	549.2
45	99	123.4	311.5	497
50	100.5	89.6	230.9	486.1
55	104.6	127.1	194.5	508.1
60	101.9	79.3	125.8	440.7
65	104.6	127.1	194.5	508.1
70	100.5	89.7	230.9	486.1
75	99	123.5	311.5	497
80	88.1	148.7	271.7	549.2
85	81.9	161.9	290.8	573.1
90	66.4	167	291.1	621.2
95	55.3	210.5	331.9	563.7
100	39.8	212.1	324.3	505.4
105	38.6	197.8	327.3	359.2
110	29.7	178.6	326.5	268.1
115	20.8	171.6	288.6	232.7
120	14	151.3	257.1	245.2

Azimuth	Total Average Power (W)			
(θ)	TSR=1	TSR=2	TSR=3	TSR=4
125	20.8	171.8	288.6	232.7
130	29.7	178.8	326.5	268.1
135	38.6	198.1	327.3	359.2
140	39.8	212.6	324.3	505.4
145	55.3	211	331.9	563.7
150	66.4	167.5	291.1	621.2
155	81.9	162.2	290.8	573.1
160	88.1	148.8	271.7	549.2
165	99	123.4	311.5	497
170	100.5	89.5	230.9	486.1
175	104.6	127	194.5	508.1
180	101.9	79.1	125.8	440.7
185	104.6	127	194.5	508.1
190	100.5	89.5	230.9	486.1
195	99	123.4	311.5	497
200	88.1	148.8	271.7	549.2
205	81.9	162.2	290.8	573.1
210	66.4	167.5	291.1	621.2
215	55.3	211	331.9	563.7
220	39.8	212.6	324.3	505.4
225	38.6	198.1	327.3	359.2
230	29.7	178.8	326.5	268.1
235	20.8	171.8	288.6	232.7
240	14	151.3	257.1	245.2
245	20.8	171.6	288.6	196
250	29.7	178.6	326.5	231.7
255	38.6	197.8	327.3	323.5
260	39.8	212.1	324.3	470.3
265	55.3	210.5	331.9	529.3
270	66.4	167	291.1	588.4
275	81.9	161.9	290.8	541.8
280	88.1	148.7	271.7	528.2
285	99	123.5	311.5	473.8

Azimuth	Total Average Power (W)			
(θ)	TSR=1	TSR=2	TSR=3	TSR=4
290	100.5	89.7	230.9	458
295	104.6	127.1	194.5	523.2
300	101.9	79.3	125.8	454.6
305	104.6	127.1	194.5	552.8
310	100.5	89.6	230.9	528.9
315	99	123.4	311.5	537
320	88.1	148.5	271.7	549.2
325	81.9	161.7	290.8	553.3
330	66.4	166.8	291.1	600.6
335	55.3	210.5	331.9	563.7
340	39.8	212	324.3	505.4
345	38.6	197.6	327.3	355.2
350	29.7	178.2	326.5	272.2
355	20.8	171.2	288.6	232.7
360	14	150.8	257.1	245.2
Average	64.5	158.5	281.4	453.2

Table A 9: Results at TSR=1, 2, 3, 4 and pitch angle of 180^{o}.

Azimuth	Total Average Power (W)			
(θ)	TSR=1	TSR=2	TSR=3	TSR=4
0	12.4	98.2	154	127.5
5	13.8	99.9	160.6	77.4
10	18.1	95.7	157.8	76.1
15	27.3	95.9	151.4	74.5
20	36.9	96.5	142	72.7
25	50.5	97	138.2	71.9
30	60.7	100.3	97.2	71.4
35	74.9	100.6	68.3	51.1
40	83.3	92.2	65.4	30.5
45	94.3	79.6	71.4	29.4
50	99.2	58.8	61.1	27.3

Azimuth	Total Average Power (W)			
(θ)	TSR=1	TSR=2	TSR=3	TSR=4
55	104.6	50.4	78.8	92.1
60	104.7	48.8	76.7	42.4
65	104.6	50.5	78.8	92.1
70	99.2	58.9	61.1	27.3
75	94.3	79.7	71.4	29.4
80	83.3	92.4	65.4	30.5
85	74.8	100.9	68.3	51.1
90	60.7	100.7	97.2	71.4
95	50.5	97.1	138.2	71.9
100	36.9	96.7	142	72.7
105	27.3	96.2	151.4	74.5
110	18.1	96.2	157.8	76.1
115	13.8	100.5	160.6	77.4
120	12.4	98.9	154	127.5
125	13.8	100.7	160.6	77.4
130	18.1	96.5	157.8	76.1
135	27.3	96.7	151.4	74.5
140	36.9	97.3	142	72.7
145	50.5	97.7	138.2	71.9
150	60.7	101.2	97.2	71.4
155	74.9	101.2	68.3	51.1
160	83.3	92.6	65.4	30.5
165	94.3	79.6	71.4	29.4
170	99.2	58.6	61.1	27.3
175	104.6	50.3	78.8	92.1
180	104.7	48.6	76.7	42.4
185	104.6	50.3	78.8	92.1
190	99.2	58.6	61.1	27.3
195	94.3	79.6	71.4	29.4
200	83.3	92.6	65.4	30.5
205	74.8	101.2	68.3	51.1
210	60.7	101.2	97.2	71.4
215	50.5	97.7	138.2	71.9

Azimuth	Total Average Power (W)			
(θ)	TSR=1	TSR=2	TSR=3	TSR=4
220	36.9	97.3	142	72.7
225	27.3	96.7	151.4	74.5
230	18.1	96.5	157.8	76.1
235	13.8	100.7	160.6	77.4
240	12.4	98.9	154	127.5
245	13.8	100.5	160.6	77.3
250	18.1	96.2	157.8	75.8
255	27.3	96.2	151.4	74.2
260	36.9	96.7	142	72.1
265	50.5	97.1	138.2	70.9
270	60.7	100.7	97.2	70.7
275	74.9	100.9	68.3	50.6
280	83.3	92.4	65.4	29.5
285	94.3	79.7	71.4	29.2
290	99.2	58.9	61.1	27.2
295	104.6	50.5	78.8	91.1
300	104.7	48.8	76.7	41.2
305	104.6	50.4	78.8	91.5
310	99.2	58.8	61.1	26.6
315	94.3	79.6	71.4	28.9
320	83.3	92.2	65.4	30.5
325	74.8	100.6	68.3	30.5
330	60.7	100.3	97.2	50.9
335	50.5	97	138.2	71.9
340	36.9	96.5	142	72.7
345	27.3	95.9	151.4	74.6
350	18.1	95.7	157.8	76.1
355	13.8	99.9	160.6	77.4
360	12.4	98.2	154	127.5
Average	59.5	87.1	109.6	63.5

Table A 10: The average power at different values of blade pitch angles at TSR=1, 2, 3, and 4.

β=f (θ)	Total Average Power (W)			
(θ)	TSR=1	TSR=2	TSR=3	TSR=4
β = 0.25 θ	0.793	-8.38	-6.234	107.882
β = 0.5 θ	1.346343	-5.30579	0.487034	122.3132
β = θ	2.6948	9.868056	7.20496	134.8319
β = 22.5 θ	-0.953	128.781	308.63	736.135
β = 45 θ	42.55	82.465	116.526	194.375
β = 67.5 θ	11.185	36.943	33.441	73.894
β = 90 θ	-11.683	6.625	57.868	154.119

Table A 11: The parameters affecting the annual energy production and capacity factor.

U, (m/s)	WP	WB	W, C_P	HP	TP	TE
	kW	kW	kW	kW	kW	kW
0	0	0	0	0	0	0
1	0.06	0.103	0.006	0	0	0
2	0.1	0.189	0.014	0	0	0
3	0.13	0.246	0.02	0.009	0.007	0.001
4	0.14	0.269	0.023	0.02	0.017	0.002
5	0.14	0.261	0.023	0.039	0.034	0.005
6	0.12	0.229	0.02	0.068	0.06	0.007
7	0.1	0.185	0.016	0.108	0.096	0.01
8	0.07	0.138	0.012	0.161	0.144	0.011
9	0.05	0.096	0.009	0.23	0.207	0.011
10	0.03	0.062	0.006	0.315	0.285	0.009
11	0.02	0.038	0.003	0.42	0.381	0.008
12	0.01	0.021	0.002	0.545	0.497	0.006
13	0.01	0.011	0.001	0.693	0.633	0.004
14	0	0.006	0.001	0.865	0.793	0.002
15	0	0.003	0	1.064	0.977	0.001
16	0	0.001	0	1.291	1.188	0.001
17	0	0	0	1.549	1.427	0
18	0	0	0	1.839	1.697	0

U, (m/s)	WP	WB	W, C_P	HP	TP	TE
	kW	kW	kW	kW	kW	kW
19	0	0	0	2.163	1.998	0
20	0	0	0	2.522	2.333	0
21	0	0	0	2.92	2.701	0
22	0	0	0	3.357	3.106	0
23	0	0	0	3.836	3.549	0
24	0	0	0	4.359	4.032	0
25	0	0	0	4.927	4.557	0

Table A 12: The annual energy production and capacity factor of the model.

Ref#	(kW)	AL	ML	AV	AEP	CF
	∑TE	(%)	(%)	(%)	(kWh)	(%)
	0.07833	0	3.5	95	896.208	19.524

Table A 13: Hub heights equal to 4 m, 6 m and 8 m at constant wind speed of 6 m/s.

U	∑TE	AL	ML	AV	AEP	CF
6 m/s (constant)	(kW)	(%)	(%)	(%)	(kWh)	(%)
H = 4 m	0.07833	0	3.5	95	896.208	19.524
H = 6 m	0.14032	0	3.5	95	1070.55	23.32
H = 8 m	0.1592	0	3.5	95	1214.15	26.45

Table A 14: Wind speeds equal to 6, 8 and 10 m/s at constant hub height of 4 m.

H, 4 m	∑TE	AL	ML	AV	AEP	CF
(constant)	(kW)	(%)	(%)	(%)	(kWh)	(%)
V= 6 m/s	0.07833	0	3.5	95	896.208	0.19524
V= 8 m/s	0.2826	0	3.5	95	2156.39	0.4698
V= 10 m/s	0.5455	0	3.5	95	4161.51	0.9066

References

[1] A. Sharma, C. Chen, and N. Vu Lan, "Solar-energy drying systems: A review," *Renew. Sustain. Energy Rev.*, vol. 13, no. 6–7, pp. 1185–1210, 2009.

[2] M. H. Mughal and L. Guojie, "Review of Pitch Control for Variable Speed Wind Turbine," in *2015 IEEE 12th Intl Conf on Ubiquitous Intelligence and Computing and 2015 IEEE 12th Intl Conf on Autonomic and Trusted Computing and 2015 IEEE 15th Intl Conf on Scalable Computing and Communications and Its Associated Workshops (UIC-ATC-ScalCom)*, 2015, pp. 738–744.

[3] M. Ó. Óskarsdóttir, "A General Description and Comparison of Horizontal Axis Wind Turbines and Vertical Axis Wind Turbines," University of Iceland, 2014.

[4] H. Kala and K. S. Sandhu, "Effect of change in power coefficient on the performance of wind turbines with different dimensions," in *International Conference on Microelectronics, Computing and Communication, MicroCom 2016*, 2016.

[5] W. Sridech and T. Chitsomboon, "Optimal speed for stall-regulated wind turbines in Thailand," *mechatronics.pit.ac.th*.

[6] A. Sunyoto, F. Wenehenubun, and H. Sutanto, "The effect of number of blades on the performance of H-Darrieus type wind turbine," in *2013 International Conference on Quality in Research, QiR 2013 - In Conjunction with ICCS 2013: The 2nd International Conference on Civic Space*, 2013, pp. 192–196.

[7] A. K. Wright and D. H. Wood, "The starting and low wind speed behaviour of a small horizontal axis wind turbine," *J. Wind Eng. Ind. Aerodyn.*, vol. 92, no. 14–15, pp. 1265–1279, 2004.

[8] I. S. Hwang, S. Y. Min, I. O. Jeong, Y. H. Lee, and S. J. Kim, "Efficiency improvement of a new vertical axis wind turbine by individual active control of blade motion," 2006, vol. 6173, p. 617311.

[9] N. Caplan and T. N. Gardner, "A fluid dynamic investigation of the Big Blade and Macon oar blade designs in rowing propulsion," *J. Sports Sci.*, vol. 25, no. 6, pp. 643–650, 2007.

[10] A. M. K. (Arnold Martin), *Foundations of aerodynamics : bases of aerodynamic design*. 1998.

[11] R. E. Sheldahl and P. C. Klimas, "Aerodynamic Characteristics of Seven Symmetrical Airfoil Section Through 180-Degree Angle of Attack for Use in Aerodynamic Analysis of Vertical Axis Wind Turbines," *Seven*, vol. SAND80-211. p. 118, 1981.

[12] D. Wood, *Small Wind Turbines*. 2011.

[13] A. M. Biadgo, A. Simonovic, D. Komarov, and S. Stupar, "Numerical and analytical investigation of vertical axis wind turbine," *FME Trans.*, vol. 41, no. 1, pp. 49–58, 2013.

[14] Y. Staelens, F. Saeed, and I. Paraschivoiu, “A Straight-Bladed Variable-Pitch VAWT Concept for Improved Power Generation,” in *ASME 2003 Wind Energy Symposium*, 2003, pp. 146–154.
[15] J. Castillo, “SMALL-SCALE VERTICAL AXIS WIND TURBINE DESIGN,” 2011.
[16] S. B. Weiss, “Vertical axis wind turbine with continuous blade adjustment,” 2010.
[17] I. Erlich and F. Shewarega, “Introduction of wind power generation into the first course in power systems,” in *2007 IEEE Power Engineering Society General Meeting, PES*, 2007.
[18] J. Decoste, D. McKay, B. Robinson, S. Whitehead, and S. Wright, “Vertical Axis Wind Turbine,” *Dep. Mech. Eng. Dalhousie Univ.*, pp. 1–77, 2005.
[19] H. Shiu, M. Milligan, B. Kirby, and K. Jackson, “California Renewables Portfolio Standard, Renewable Generation Integration Cost Analysis - Multi-year analysis results and recommendations final report,” 2006.
[20] J. O. G. Tande and M. Korpås, “Impact of offshore wind power on system adequacy in a regional hydro-based power system with weak interconnections,” in *Energy Procedia*, 2012, vol. 24, pp. 131–142.
[21] L. Söder and M. Amelin, “A review of different methodologies used for calculation of wind power capacity credit,” in *IEEE Power and Energy Society 2008 General Meeting: Conversion and Delivery of Electrical Energy in the 21st Century, PES*, 2008.
[22] A. D. Mills, “The Cost of Transmission for Wind Energy: A Review of Transmission Planning Studies.” 2009.
[23] H. Holttinen, P. Saarikivi, S. Repo, J. Ikäheimo, and G. Koreneff, “Prediction Errors and Balancing Costs for Wind Power Production in Finlands,” in *Proceedings of the 6th International Workshop on Large-Scale Integration of Wind Power and Transmission Networks for Offshore Wind Farms*, 2006.
[24] P. Meibom, C. Weber, R. Barth, and H. Brand, “Operational costs induced by fluctuating wind power production in Germany and Scandinavia,” *IET Renew. Power Gener.*, vol. 3, no. 1, p. 75, 2009.
[25] J. P. Dismukes, L. K. Miller, A. Solocha, S. Jagani, and J. A. Bers, “Wind Energy Electrical Power Generation: Industrial Life Cycle of a Radical Innovation,” in *PICMET ’07 - 2007 Portland International Conference on Management of Engineering & Technology*, 2007, pp. 773–785.
[26] D. J. Malcolm and A. C. Hansen, “WindPACT Turbine Rotor Design Study,” 2006.
[27] Global Energy Concepts, “WindPACT Turbine Design Scaling Studies Technical Area 3 – Self-Erecting Tower and Nacelle Feasibility,” *Energy*, no. May, 2001.
[28] D. a Griffin, “WindPACT Turbine Design Scaling Studies Technical Area 1 - Composite Blades for 80-to 120-Meter Rotor.,” *Natl. Renew. Energy Lab. NREL/SR-500 ...*, no. April, 2001.
[29] G. Bywaters, V. John, J. Lynch, P. Mattila, G. Norton, J. Stowell, M. Salata, O.

Labath, A. Chertok, and D. Hablanian, “Northern Power Systems WindPACT Drive Train Alternative Design Study Report Northern Power Systems WindPACT Drive Train Alternative Design Study Report,” *Nrel*, no. October 2004, 2005.

[30] W. Musial and B. Ram, “Large-Scale Offshore Wind Power in the United States: Assessment of Opportunities and Barriers,” 2010.

[31] J. V. Seguro and T. W. Lambert, “Modern estimation of the parameters of the Weibull wind speed distribution for wind energy analysis,” *J. Wind Eng. Ind. Aerodyn.*, vol. 85, no. 1, pp. 75–84, Mar. 2000.

[32] C. D. Lai, M. Xie, and D. N. P. Murthy, “A modified Weibull distribution,” *IEEE Trans. Reliab.*, vol. 52, no. 1, pp. 33–37, 2003.

[33] A. R. El-Baz, K. Youssef, and M. H. Mohamed, “Innovative improvement of a drag wind turbine performance,” *Renew. Energy*, vol. 86, pp. 89–98, 2015.

[34] R. H. Crawford, “Life cycle energy and greenhouse emissions analysis of wind turbines and the effect of size on energy yield,” *Renew. Sustain. Energy Rev.*, vol. 13, no. 9, pp. 2653–2660, 2009.

[35] L. Fingersh, M. Hand, and A. Laxson, “Wind Turbine Design Cost and Scaling Model Wind Turbine Design Cost and Scaling Model,” 2006.

[36] D. A. Shafer, K. R. Strawmyer, R. M. Conley, G. J. H, D. C. Wilkie, and T. F. Zellman, “WindPACT Turbine Design Scaling Studies: Technical Area 4 -- Balance-of-Station Cost,” 2001.

VITAE

Personal Information

Name: Mudhafar Ali Hasan Mudhafar

Marital Status: Married with two children (Aalaa & Aseel)

Nationality: Yemeni

Date of Birth: 1st January 1985

Permanent Address: Al-Jameemah, Ans, Dhamar City, Yemen

Email: mmudhafar@ymail.com

Mobile: +966-55-941-7279 & +967-774-826-789

Educational Qualification

- Graduated from high school in 2003, scientific stream, Ogbah Ben Nafaa Secondary Boys School (2002-2003), Dhamar, Yemen.
- B.Sc. in Mechanical Engineering, Tishreen University, September 2004-September 2009, Lattakia-Syria.
- Received a scholarship from the Ministry of Higher Education and Tishreen University to join summer training for students of high score (2007), Munich, Germany.

- Received a scholarship from the Ministry of Higher Education and Thamar University to study M.S degree at KFUPM in 2015.
- M.S (Mechanical Engineering & Thermal Science), King Fahd University of Petroleum and Minerals, September 2015-Jan, 2018, Dhahran, Saudi Arabia.

Work and Experience

- In 2009, Assigned as as an Instructor at Thamar University in Yemen, College of Engineering and I am still working there as a faculty member.
- During the period from 2010 to 2015, I visited many power plants in Yemen.

Publication / Conference Attendance

- **Mudhafar Mudhafar**, Ahmet Z. Sahin, Haitham Bahaidarah, and Hassen Ouakad "Cost and performance evaluation of a large-scale wind turbine in Yemen".

  Status: In Progress.

- **Mudhafar Mudhafar**, Ahmet Z. Sahin, Haitham Bahaidarah, and Hassen Ouakad “Optimization of torque and power produced from a small scale vertical axis wind turbine”

  Status: In Progress.

- **Mudhafar Mudhafar**, Ahmet Z. Sahin, Haitham Bahaidarah, and Hassen Ouakad “Simulation and economic analysis of a photovoltaic system in Saudi Arabia”.

  Status: In Progress.